Int. J. Heat Mass Transfer. Vol. 12, pp. 1353–1384. Pergamon Press 1969. Printed in Great Britain

INVESTIGATIONS ON THE CRITICAL HEAT FLUX OF PURE LIQUIDS AND MIXTURES UNDER VARIOUS CONDITIONS

S. J. D. VAN STRALEN† and W. M. SLUYTER‡
Heat Transfer Section, Technological University, Eindhoven, The Netherlands

(*Received* 23 *December* 1968)

Abstract—The effects of the diameter and of the orientation of electrically heated wires on their critical heat flux, both in saturated pool boiling and in surface boiling, have been investigated.

A minimum in the peak flux on horizontal wires in saturated boiling occurs at a diameter of 100 μm. The peak flux at diminishing diameter increases rapidly as a consequence of a corresponding increase in the convective heat transfer. A similar effect has been observed in surface boiling, where the slope of the peak flux vs. subcooling curves for horizontal wires increases at decreasing wire diameter.

Generally, the critical heat flux on horizontal wires in pure liquids exceeds the value on vertical wires. This is caused by a premature onset of film boiling in the latter case by the formation of vapour slugs at the upper end of the heater. Contrarily, the considerably higher peak fluxes occurring in certain binary mixtures (in coincidence with a slowing down of bubble growth at low concentrations of the more volatile component) are practically independent of the orientation of the heating element, because the Marangoni-effect diminishes the possibility of bubble coalescence.

A quite different behaviour of the peak flux is observed on wires and strips, which are surrounded by a narrow coaxial tube: higher values occur on vertical heating elements now, as the possibility for bubbles to escape from the inside of the tube is minimized in the horizontal position.

Some preliminary investigations on the peak flux in saturated pool boiling of aqueous ternary mixtures show the existence of a direct relationship to the behaviour of the basic aqueous binary mixtures.

NOMENCLATURE

a, liquid thermal diffusivity, $= k/\rho_1 c$ [m^2/s];
A_w, area of heating surface [m^2];
b, dimensionless bubble growth parameter;
B, coefficient in platinum temperature equation [deg C^{-1}];
c, liquid specific heat at constant pressure [J/kg deg C];
C, coefficient in platinum temperature equation [deg C^{-2}];
C_1, bubble growth constant, for relatively large liquid superheatings [$m/s^{\frac{1}{2}}$ deg C];
d, instantaneous thickness of relaxation microlayer, or of equivalent conduction layer [m];
D, mass diffusivity of more volatile component in less volatile component [m^2/s];
D_t, inner diameter of coaxial glass tube surrounding heating wire [m];
D_w, diameter of heating wire [μm or m];
e, base of natural logarithms (2·718 ...);
E, effective potential drop across heating wire [V];
g, gravitational acceleration [m/s^2];
G_d, vaporized mass diffusion fraction for individual bubble;

† Doctor of Physics, Principal Research Scientist.
‡ Research Assistant.

Gr, Grashof number;
I, effective electrical current strength through heating wire [A];
k, liquid thermal conductivity [W/m deg C];
K, equilibrium constant of more volatile component in binary mixture (ratio of mass fractions), $= y/x$;
l, latent heat of vaporization [J/kg];
L_w, length of heating wire [m];
m, dimensionless number of active nuclei generating bubbles on entire area A_w of heating surface;
m/A_w, number of active nuclei on unit area of heating surface, or nuclei density [m^{-2}];
n, $= 1/\theta_{o,p,max}$ [deg C^{-1}];
Nu, Nusselt number;
Pr, Prandtl number;
q, rate of heat flow through unit area, or heat flux density [W/m^2];
R_T, electrical resistance of platinum wire at boiling temperature of liquid [Ω];
$R_{T+\theta_0}$, electrical resistance of platinum wire at superheating θ_0 [Ω];
R_1, $= R(t_1)$, (equivalent) bubble radius at the instant t_1 of breaking away from heating surface [m];
S, $= (D_t - D_w)/4R_1$, dimensionless number;
t, time elapsed since initial bubble formation during adherence [s];
t_1 instant at which bubble is breaking away from heating surface, or departure time [s];
t_2, delay, or waiting time between formation of succeeding bubble on same nucleus and departure of bubble [s];
T, boiling point, or saturation temperature at ambient pressure [deg C];
$T(x)$, boiling temperature of liquid at bubble boundary in binary liquid mixture [deg C];
$T(x_{0,1})$, boiling temperature of original liquid in binary mixture [deg C];
$T(x_{0,1})$, boiling temperature of original liquid at constant $x_{0,2}$ in ternary mixture [deg C];
$T(x_{0,2})$, boiling temperature or original liquid at constant $x_{0,1}$ in ternary mixture [deg C];
$T(y)$, dew temperature of saturated vapour in binary mixture, $T(y) = T(x)$ [deg C];
T_0, temperature of bulk liquid in surface boiling [deg C];
ΔT, temperature difference between dew temperature of vapour bubbles and boiling temperature of original liquid in binary mixture, or increase in temperature of liquid at bubble boundary with respect to original liquid, $\Delta T = 0$ for pure liquid and for azeotropic mixture, $= T(y) - T(x_0) = T(x) - T(x_0)$ [degC];
x, mass fraction of more volatile component in liquid at bubble boundary in binary mixture, $= x_0/\{1 + (K - 1)G_d\}$;
x_0, mass fraction of more volatile component in original liquid in binary mixture;
$x_{0,1}$, mass fraction of volatile organic component at constant $x_{0,2}$ in ternary mixture;
$x_{0,2}$, mass fraction of volatile organic component at constant $x_{0,1}$ in ternary mixture;
y, mass fraction of more volatile component in vapour of binary mixture.

Greek letters

γ, coefficient of cubical expansion of liquid [deg C^{-1}];
η, liquid dynamic viscosity [kg/sm];
θ_0, superheating of heating surface, or initial maximum superheating of relaxation microlayer surrounding part of bubble boundary [deg C];

θ_0^*, difference between saturation temperature and temperature of bulk liquid in surface boiling or (degree of) subcooling, $= T - T_0$ [deg C];
ν, frequency of bubble formation on nucleus [1/s];
ρ_1, liquid density [kg/m^3];
ρ_2, saturated vapour density [kg/m^3];
σ, surface tension constant [kg/s^2];
φ, ϕ, angle between axis of heating wire and horizontal plane;
$\psi(T)$, multiplication factor in equation for superheating of platinum heating wire [deg C];

Subscripts

b, (for heat flux density) applying to direct vapour formation at heating surface;
bi, (for heat flux density) bubble-induced contribution, or difference between total heat flux and convection contribution, $q_{w,bi} = q_w - q_{w,co}$, $q_{w,b} < q_{w,bi}$ in mixture, $q_{w,b} = q_{w,bi}$ in pure liquid;
co, (for heat flux density) actual convection contribution or contribution due to free convection;
m, value in binary mixture;
max, value for peak flux conditions;
0, maximum value (exceptions: T_0 and x_0);
p, value in less volatile pure component;
w, value for heating surface.

Superscript

*, value for surface boiling of subcooled liquid.

Numerical constants at atmospheric pressure and boiling point

Water

a, $= 16{\cdot}9 \times 10^{-8}$ m^2/s;
c, $= 4216$ J/kg deg C;
$C_{1,p}$, $= 24 \times 10^{-4}$ m/s$^{\frac{1}{2}}$ degC;
g, $= 9{\cdot}81$ m/s^2;
Gr, $= \frac{\rho_1^2 \gamma g}{\eta^2}[L^3]\theta_0 = 8{\cdot}643 \times 10^{10}[L^3]\theta_0$;
k, $= 0{\cdot}6825$ W/m deg C;
l, $= 22{\cdot}56 \times 10^5$ J/kg;
Nu, $= \frac{q_{w,co,p}}{k}\frac{[L]}{\theta_0} = 1{\cdot}465\, q_{w,co,p}\frac{[L]}{\theta_0}$;
Pr, $= \frac{c\eta}{k} = 1{\cdot}75$;
T, $= 100$ deg C;
γ, $= 7{\cdot}52 \times 10^{-4}$ degC^{-1};
ρ_1, $= 958{\cdot}4$ kg/m^3;
ρ_2, $= 0{\cdot}598$ kg/m^3;
σ, $= 0{\cdot}0587$ kg/s^2.

1-Butanol

a $= 6{\cdot}40 \times 10^{-8}$ m^2/s;
c $= 3469$ J/kg deg C;
k $= 0{\cdot}1621$ W/m deg C;
l $= 5{\cdot}89 \times 10^5$ J/kg;
T $= 118$ deg C;
ρ_1 $= 730$ kg/m^3;
ρ_2 $= 2{\cdot}72$ kg/m^3;
σ $= 0{\cdot}0175$ kg/s^2.

Water–1-butanol: $x_0 = 1{\cdot}5 \times 10^{-2}$

$(a/D)^{\frac{1}{2}}$ $= 13{\cdot}1$;
$C_{1,m}$ $= 18 \times 10^{-4}$ m/s$^{\frac{1}{2}}$ deg C; 9×10^{-4} m/s$^{\frac{1}{2}}$ deg C for adhering bubbles generated on "complex nuclei";
D $= 9{\cdot}9 \times 10^{-10}$ m^2/s;
T $= 97$ degC;
$(\Delta T/G_d)_0$ $= 35$ deg C.

Water–methylethylketone: $x_0 = 4{\cdot}1 \times 10^{-2}$

$(a/D)^{\frac{1}{2}}$ $= 13{\cdot}2$;
$C_{1,m}$ $= 6 \times 10^{-4}$ m/s$^{\frac{1}{2}}$ deg C;
D $= 9{\cdot}7 \times 10^{-10}$ m^2/s;
T $= 88$ deg C;
$(\Delta T/G_d)_0$ $= 180$ deg C.

Water–ethanol: $x_0 = 20 \times 10^{-2}$
$(a/D)^{\frac{1}{2}} = 11{\cdot}4$;
$C_{1,m} = 16 \times 10^{-4}\ \mathrm{m/s^{\frac{1}{2}}\ deg\ C}$;
$D = 12{\cdot}9 \times 10^{-10}\ \mathrm{m^2/s}$;
$T = 86\ \mathrm{deg\ C}$;
$(\Delta T/G_d)_0 = 35\ \mathrm{deg\ C}$.

INTRODUCTION

ONLY a few data of the effect of the orientation and of the dimensions of the heating surface on the nucleate boiling peak flux density, $q_{w,max}$, are known in the literature.

The present study includes a systematic investigation of this behaviour on electrically heated wires both for saturated pool boiling and for surface boiling of water and some aqueous binary mixtures. The investigated mixtures contain a low concentration of the more volatile organic component, at which a striking coincidence occurs of a maximal peak flux and a minimal bubble growth rate, cf. [1–3].

The effect of the inner diameter of a coaxial glass tube surrounding a heating wire in saturated boiling is studied extensively. This topic is a special case of two-phase flow, approximating the conditions of free convection; the riser consists here of the space inside the tube, and the downcomer is extended to the entire bulk liquid in the boiling vessel (Fig. 1).

The applied construction of the vessel provides for a combination with orientation. In order to obtain a better reproducibility of the results, the same heating wire can be used in an arbitrary position between horizontal and vertical, as the axis of the wire can be adjusted by operating the drawbars from the outside of the vessel.

A different behaviour of binary mixtures with a low concentration of the more volatile component and pure liquids is predicted to occur in this case also, as a consequence of the slowing down of bubble growth in these mixtures.

1. BOILING CURVES

1.1. *Procedure*

In most cases, the heating surface consisted of an electrically heated "physically pure" (99·99%) platinum wire, which acted at the same time as a resistance thermometer [1, 3]. Preference is given to a.c. heating instead of d.c. to avoid fouling due to electrolysis.

In this way, boiling curves, $q_w(\theta_0)$, can be determined easily, as the heat flux density can be calculated from the electric power:

$$q_w = \frac{EI}{\pi L_w D_w}. \tag{1}$$

The average superheating of the wire surface follows from the quadratic resistance equation for platinum:

$$\theta_0 = \psi(T)\left(\frac{R_{T+\theta_0}}{R_T} - 1\right) + \frac{C}{B - 2CT} \times \left[\psi(T)\left(\frac{R_{T+\theta_0}}{R_T} - 1\right)\right]^2 - \frac{D_w}{8k} q_w, \tag{2}$$

where $R_{T+\theta_0} = E/I$ denotes the electrical resistance of the wire and R_T a reference value, i.e. the resistance at the boiling temperature T (in °C) of the liquid. The wires have previously been annealed at red heat in air for 15 min. The factor

$$\psi(T) = \frac{1 + BT - CT^2}{B - 2CT}, \tag{3}$$

where the coefficients in the resistance equation $B = 3{\cdot}9788 \times 10^{-3}\ °C^{-1}$ and $C = 5{\cdot}88 \times 10^{-7}\ °C^{-2}$.

Both the effective potential drop E across the wire and the effective current strength I were recorded simultaneously on universal digital voltmeters (accurate to 10 μV) by connecting a standard-resistor of maganin (0·03%) in series with the wire. The resistance of the nickel-coated copper electrodes or of the flexible aluminium supply-wires was taken into account.

1.2. *Water*

1.2.1. *Complete curve for horizontal wire*

The boiling curve on a horizontal platinum wire for water at atmospheric pressure is shown in Fig. 2. The transition to the region of film

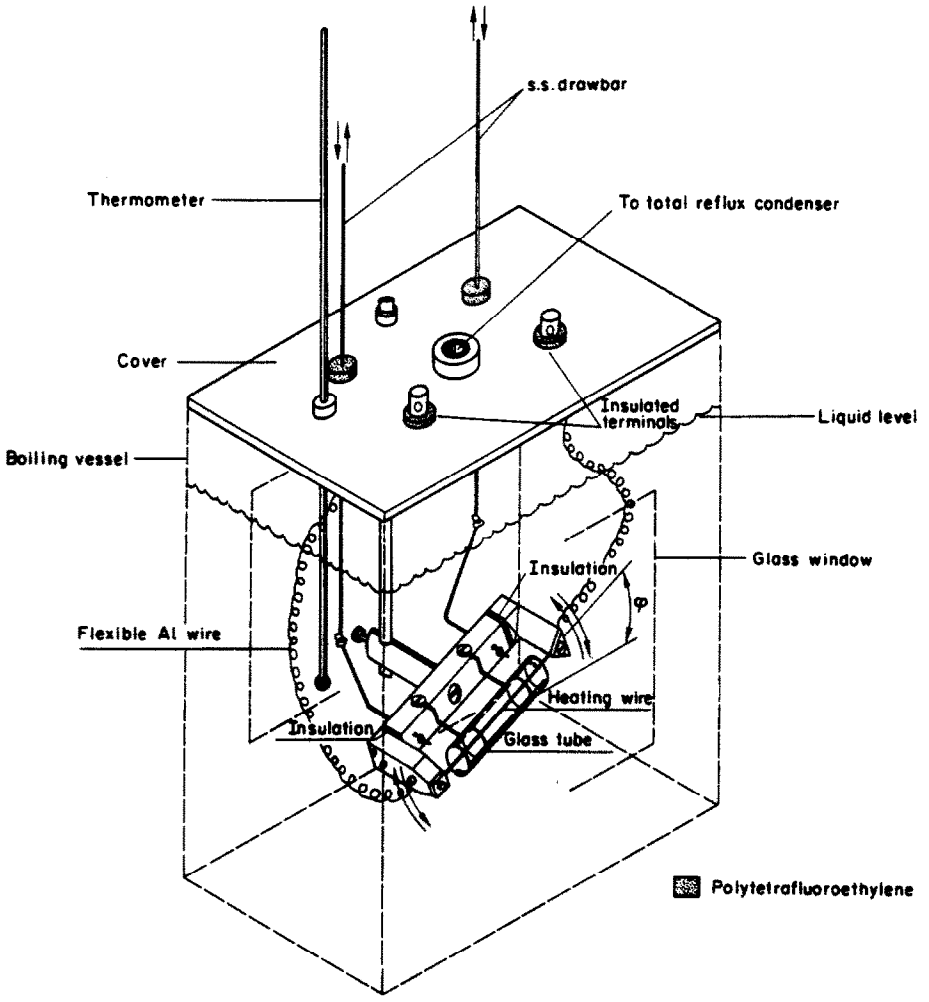

FIG. 1. Boiling vessel with rotatable electrically heated test wire and coaxial glass tube.

boiling occurs at the critical $\theta_{0,\max}$. This transition corresponds with a decrease in heat flux as a consequence of the increase in the resistance of the wire.

Burnout in film boiling occurs for similar platinum wires at a heat flux, which amounts to 1·8 times the nucleate boiling peak flux density $q_{w,p,\max}$. A limited number of large vapour bubbles is generated in film boiling. At decreasing wire superheating θ_0 the Leidenfrost-point is passed at a minimum heat flux of 0·55 times the nucleate boiling peak flux. The reference value R_T [cf. the right-hand side of equation (2) in which the first term is dominating] has been increased during film boiling; this is probably due to an inelastic extension of the wire. Consequently, the values of θ_0 in nucleate boiling at decreasing heat flux, which are based on the original value of R_T, are too high. A correction, by which the final value of R_T is substituted in equation (2) gives satisfactory results, also in the region of convection.

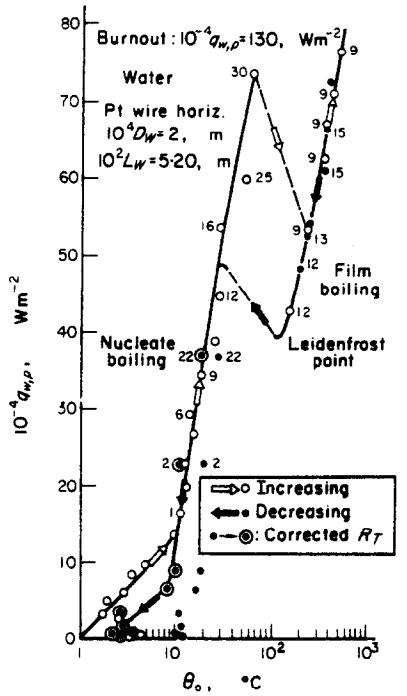

FIG. 2. *Water.* Boiling curve at atmospheric pressure. Figures at curve denote number of active nuclei generating vapour bubbles on a square cm of heating area.

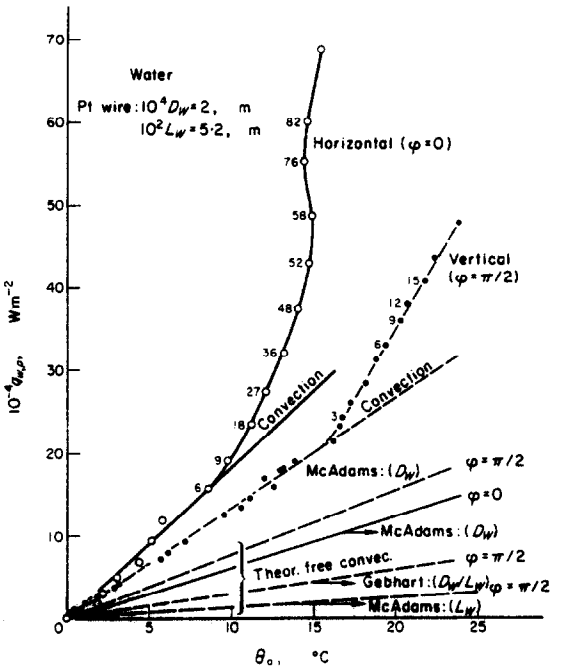

FIG. 3. *Water.* Boiling curves for convection (combination of free and forced) and nucleate boiling on horizontal and vertical wires. Figures at curves denote number of active nuclei generating vapour bubbles on a square cm of heating area.

Bottom curves denote corresponding convective heat transfer for free convection only; the characteristic dimension is placed between parentheses. Recommended curves are: McAdams [D_w] for $\phi = 0$ and Gebhart [D_w/L_w] for $\phi = \pi/2$.

1.2.2. *Effect of orientation on convection and nucleate boiling for horizontal and vertical wires*

1.2.2.1. *Region of nucleate boiling.* Figure 3 shows the boiling curves on the same platinum wire, in the horizontal ($\phi = 0$) and in the vertical position ($\phi = \pi/2$), respectively. The peak flux density $q_{w,p,\max}$ for $\phi = 0$ is 45 per cent higher in comparison to the corresponding value for $\phi = \pi/2$. The contribution $q_{w,p,bi,\max}$ [$= q_{w,p,\max} - q_{w,p,co,\max}$, cf. equation (2)], which is due to the presence of vapour bubbles, has been increased with not less than a factor of 2·7.

Apparently, this effect must be attributed to the growth of the maximal number of active nuclei per unit area or maximal density, $m_{\max}/A_w$, which increased from approximately 25×10^{-4} m^{-2} to 90×10^{-4} m^{-2}. The reduction in the maximal number of active sites for the vertical position is caused by a premature onset of film boiling at the upper part of the wire due to the formation of large vapour slugs. In this case, the coalescing bubbles originate from nuclei, which are distributed over the entire heating surface. This behaviour differs strikingly from that for a horizontal wire, where bubble coalescence is generally restricted to nearby nuclei.

1.2.2.2. *Region of convection.* The region of convection (i.e. the lower part of the boiling curves in Fig. 3) will be considered now: the convection is here a combination of free convection on the wire and forced convection arising from moving liquid, which is heated at the bottom plate of the boiling vessel (Fig. 1) and is flowing normal to the wire, with a velocity of approximately 5×10^{-2} m/s. At present, the experimental convective heat transfer can be

compared only with the contribution of the free convection.

(i) *Horizontal wire* ($\phi = 0$). McAdams [4] presented a graphical relation between Nu and $(Gr \,.\, Pr)$ for horizontal heating cylinders, which is deduced from a very large number of experimental data, both on liquids and gases. For water, the following equation is recommended for $10^3 < (Gr \,.\, Pr) < 10^9$:

$$Nu = 0{\cdot}53\,(Gr \,.\, Pr)^{0{\cdot}25}. \tag{4}$$

The diameter D_w has to be taken for the characteristic length in Nu and Gr, whence equation (4) is simplified to:

$$q_w = 0{\cdot}53 \left(\frac{\rho_1^2 c\gamma g k^3}{\eta}\right)^{0{\cdot}25} \frac{\theta_0^{1{\cdot}25}}{D_w^{0{\cdot}25}} \tag{5}$$

Actually, however, one has for $D_w = 5$–200 μm, and $5°C \leqslant \theta_0 \leqslant 20°C$, $10^{-11} < (Gr \,.\, Pr) < 25$, whence equation (5) is not valid for these thin wires. In this range, the proportionality $q_w \sim D_w^{-0{\cdot}25}$ is replaced by a similar proportionality, but with an exponent in the range from $-0{\cdot}25$ to $-0{\cdot}75$, cf. Figs. 4 and 5. For $(Gr \,.\, Pr) \sim 10^{-3}$ $q_w \sim \theta_0^{1{\cdot}08}$ instead of $q_w \sim \theta_0^{1{\cdot}25}$.

(ii) *Vertical wire* ($\phi = \pi/2$). Actually, one has to take L_w for the characteristic length in this case. However, equation (5) is giving now too small values. However, by taking D_w, the convective contribution should exceed the value for $\phi = 0$, which contradicts the experimental results. As the vertical plate solution for natural convection is predicting results for cylinders of small diameter, which are considerably below the proper values, Gebhart [5] collected data on various gases including air. Nu is plotted as a function of $(Gr \,.\, Pr)D_w/L_w$, where Gr is based on D_w. This approximation seems to give also quite satisfactory results for water (Fig. 3), as may be expected.

Obviously, the occurrence of a higher nucleate boiling peak flux on a horizontal wire is not only due to an increased maximal bubble population (the main cause), but also partly to a higher convective contribution.

1.2.3. *Effect of diameter on boiling curve for horizontal wires*

Boiling curves in convection and nucleate boiling for water at atmospheric pressure are shown in Fig. 4, the corresponding heat transfer curves for free convection [cf. Section 1.2.2.2 (i)] in Fig. 5. The curves in Fig. 5 are calculated by taking constant numerical values of the concerning termal properties, i.e. the values at 100°C.

The maximal density of active nuclei, m_{max}/A_w, increases for decreasing D_w. However, it may be useful to consider also the number, m_{max}, of nuclei, which are actually active at the entire area of the heating surface. This number follows by multiplying m_{max}/A_w by $\pi L_w D_w$, i.e. the values for $D_w = 200$, 100, 50, 25 and 10 μm by a factor of 3, 6, 12, 24 and 110, respectively, e.g. maximal only 3 nuclei are active on the 10 μm wire.

The occurrence of only one vapour bubble causes burnout of the 5 μm wire, cf. the value of the burnout heat flux in Fig. 2, and [4]. A similar behaviour—but transition to film boiling at a 6 times lower $q_{w,p,max}$ (cf. Section 8 and Fig. 10 of Part III of [2]) has been observed previously for 200 μm wires in water boiling at a subatmospheric pressure of 0·13 bar (a.). In that case the ratio $R_{1,p}/D_w = 55 \times 10^4/2 \times 10^{-4} = 27{\cdot}5$.

Obviously, the average departure radius $R_{1,p}$ of vapour bubbles decreases considerably for diminishing D_w. This behaviour has been observed actually, and is in good agreement with Van Stralen's "relaxation microlayer" theory for the mechanism of nucleate boiling. Therefore, it follows from equation (35) of Part I of [2] in combination with equations (27) and 28) of Part II of [2], that the initial, maximal thickness of the relaxation microlayer is given by the expression:

$$d_{o,p} = \left(\frac{12}{\pi} a t_{1,p}\right) = 0{\cdot}79 \frac{k\theta_0}{q_{w,co,p}}. \tag{6}$$

It is seen from equation (6), that at constant θ_0 = the ratio

$$(t_{1,p}^{\ddagger})_{D_w = 5\,\mu m}/(t_{1,p}^{\ddagger})_{D_w = 200\,\mu m} = (d_{0,p})_{D_w = 5\,\mu m}/(d_{0,p})_{D_w = 200\,\mu m} = (q_{w,co,p})_{D_w = 20\,\mu m}/(q_{w,co,p})_{D_w = 5\,\mu m}.$$

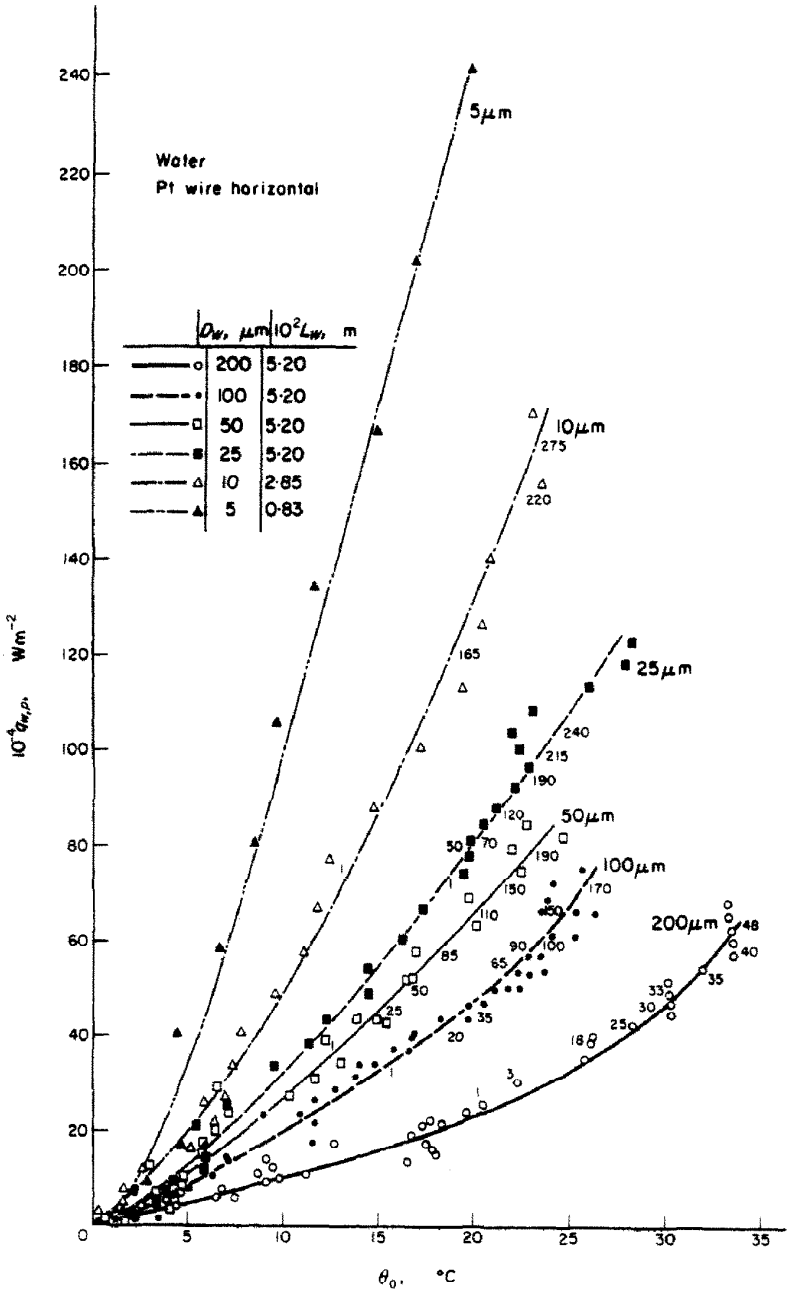

FIG. 4. *Water.* Boiling curves for convection (combination of free and forced) and nucleate boiling on horizontal wires of various diameters, cf. Figs. 5 and 6. Figures at curves denote number of active nuclei generating vapour bubbles on a square cm of heating area.

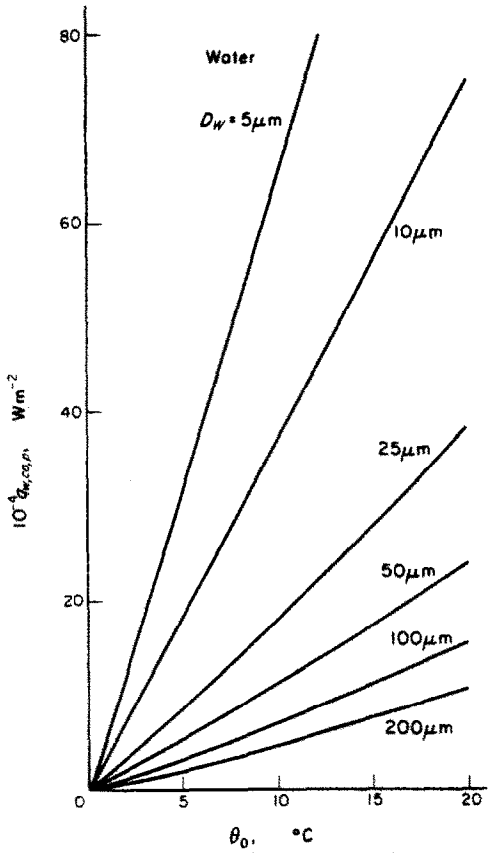

FIG. 5. *Water.* Heat transfer in free convection at atmospheric boiling point on horizontal wires of various diameters, D_w, according to McAdams, taking $[D_w]$ as characteristic dimensions, cf. Figs. 4 and 25.

Substitution of the experimental values of Fig. 5 yields for $\theta_0 = 20°C$ a ratio of $23 \times 10^4 / 240 \times 10^4 = 0{\cdot}10$. Equation (45) of Part I of [2] yields in combination with the average value $b = 0{\cdot}71$ in water (cf. Table 1 of Part I of [2]):

$$R_{1,p} = (b/e)C_{1,p}\theta_0 t_{1,p}^{\frac{1}{4}} = 0{\cdot}26\, C_{1,p}\theta_0 t_{1,p}^{\frac{1}{4}} \qquad (7)$$

Hence, the theory predicts a decrease in $R_{1,p}$ from $9{\cdot}2 \times 10^{-4}$ m (cf. Table 3 of Part II of [2] and Appendix-3 of Part III of [2]), for wires with $D_w = 200$ μm to approximately 1×10^{-4} m for wires with $D_w = 5$ μm.

The ratio $R_{1,p}/D_w$ increases from a value of 4·6 for $D_w = 200$ μm to a value of approximately 50 for $D_w = 5$μm.

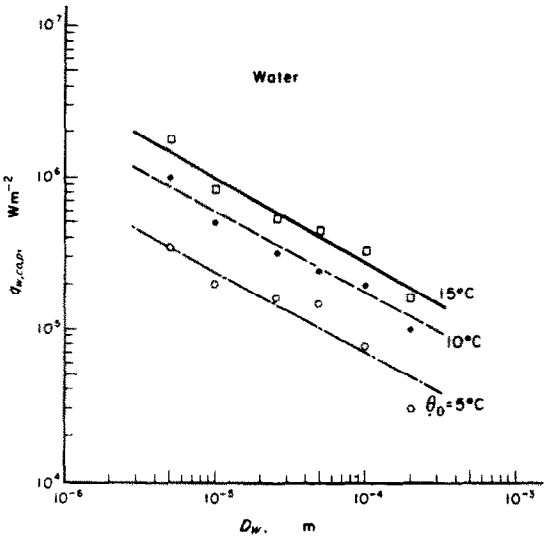

FIG. 6. *Water.* Heat transfer in convection (combination of free and forced, cf. the lower part of the curves in Fig. 4) in dependence on diameter of horizontal wire for various superheatings.

One can try to obtain a similar result by estimating the ratio of m_{max}/A_w for these wires by applying equation (64) of Part (II) of [2]:

$$\frac{m_{max}}{A_w} = \frac{3(e-1)}{4\pi b R_{1,p}^2}. \qquad (8)$$

Equation (8) predicts an increase of m_{max}/A_w with a factor of 100 by decreasing D_w from 200 μm to 5 μm. Actually, however, a factor of 15 (corresponding with a decrease of $R_{1,p}$ with a factor of 4) follows from the experimental data (Fig. 4). Although this is only a rough estimation, the effect is explained qualitatively; a deviation of a factor of 2·5 is obviously due to the fact, that $q_{w,p,max}$ is practically independent of L_w, but m_{max}/A_w is inversely proportional to L_w.

It is seen by comparing corresponding curves in Figs. 5 and 4, that—at $\theta_0 = 15°C$—the contribution due to free convection amounts to 58%, 64%, 52%, 39%, 36% and 46% of the total convective heat transfer for $D_w = 5$, 10, 25, 50, 100 and 200 μm, respectively. The electric power of the bottom heater had been kept constant during carrying out these experiments. The total convective heat transfer $q_{w,p,co}$ is shown in

Fig. 7 in dependence on wire diameter for $\theta_0 =$ 5,* 10 and 15°C. The curves, straight lines, are deduced from Fig. 4. It follows from the slope of the lines, that one has for the combined free and forced convection, that $q_{w,p,co} \sim D_w^{-0.55}$ in the range from 5–200 μm. The value of the exponent is in good agreement with the corresponding average value for free convection in this range of diameters [cf. Section 1.2.2.2 (i)].

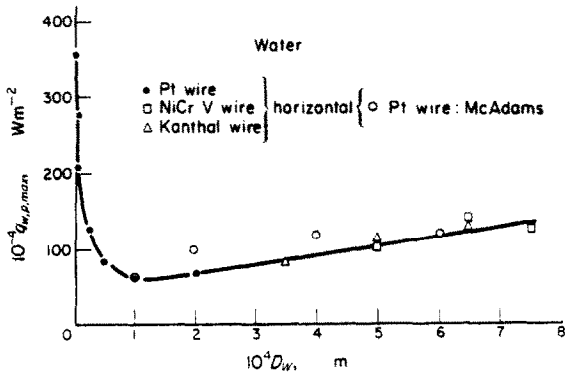

FIG. 7. *Water.* Nucleate boiling peak flux on various horizontal wires in dependence on wire diameter.

1.2.4. *Effect of diameter on peak flux for horizontal wires*

Figure 7 shows the nucleate boiling peak flux as a function of wire diameter. The curve shows a minimum value for $D_w = 100$ μm. A gradual increase of the peak flux occurs for increasing larger diameters, up to a factor of 2 at $D_w = 750$ μm.

Strikingly, the peak flux increases very rapidly for decreasing smaller diameters, up to a factor of 6 at $D_w = 3$ μm. Apparently, this behaviour is due to a corresponding increase in the convective contribution (Section 1.2.3. and Figs. 4 and 5).

The peak flux on unoxidised wires is practically independent of the composition of the heat-metal, as the values for two different alloys deviate only slightly from those for platinum.

Cole and Shulman [6] studied pool boiling of toluene at a subatmospheric pressure of 0·16 bar(a.) on horizontal (10 cm × 0·30 cm) zirconium ribbons having thicknesses of 125 μm, 250 μm and 1250 μm, respectively. Their results on the relative critical heat flux in dependence on ribbon thickness are in good agreement with those obtained previously by Bernath on tubes with constant outer diameter: the heat flux increases gradually from a low value for increasing wall thickness, rapidly for thin walls, and more slowly for thicker walls. This behaviour is attributed to the heat capacity of the heating material; a thick wall reduces the possibility of premature local burnout. This may also explain the above mentioned gradual increase of the peak flux on wires in the range from 100–750 μm (Fig. 7).

At first sight, this result seems to contradict the data plotted in Fig. 7. But, in fact, one has to consider, that in the latter experiments the convective heat transfer is constant due to the use of

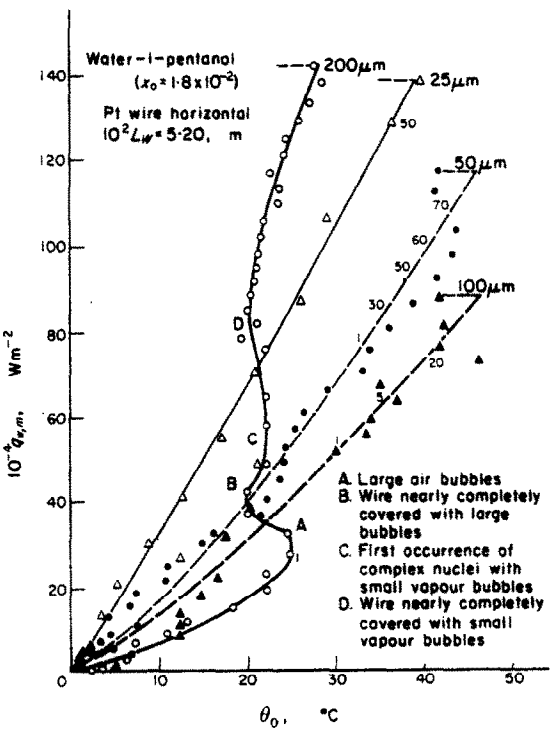

FIG. 8. *Water–1-pentanol* (1·8 *wt* % 1-*pentanol*). Boiling curves for convection (combination of free and forced) and nucleate boiling on horizontal wires of various diameters. Figures at curves denote number of active "complex nuclei" generating vapour bubbles on a square cm of heating area.

tubes with the same outer diameter or of ribbons, also with constant A_w. As a consequence, the peak flux is determined only by the behaviour of vapour bubbles, and thus by the capacity of the tube material to avoid local burnout. Contrarily, the peak flux on very thin wires is determined by the considerably increased convection.

1.3. *Binary mixtures*

1.3.1. *Effect of diameter on boiling curve for horizontal wires in* 1·8 *wt* % 1-*pentanol*

The boiling curves in Fig. 8 are in certain respects similar to those for water (Fig. 4): the convective heat transfer increases for decreasing superheating $\theta_0 = 25°C$, cf. also Sections 5 and 6 of Part III of [2]. Large bubbles, probably containing air to a considerable degree, are generated on the wire at low frequencies. At increasing heat flux, these bubbles disappear, and the wire is gradually covered with very small vapour bubbles, generated on "complex nuclei" at very high frequencies. Each complex nucleus is formed by a number of very nearby active sites, generating bubbles, cf. [2]. Bubble coalescence is prevented due to the Marangoni-effect in this "positive" mixture [2].

(ii) Curiously, the peak flux on a 100 μm wire exceeds the corresponding value in water (Fig. 4) with only 10 per cent, and is reached at a

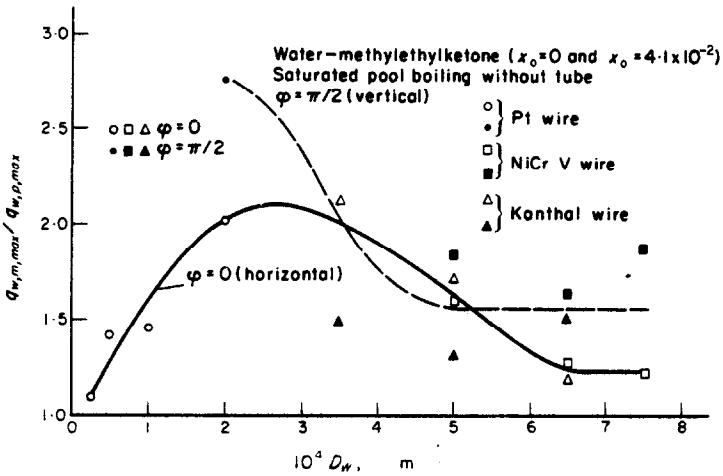

FIG. 9. *Water–methylethylketone* (4·1 *wt* % *methylethylketone*). Relative nucleate boiling peak flux in mixture in comparison to water on various wires in dependence on wire diameter.

wire diameter. The peak flux on a 200 μm wire exceeds the corresponding value in water considerably (a factor of 2·2) more or less in agreement with previous observations (a factor of 3.1, cf. [1]). The lower peak flux of the present investigation is due to the absence of active nuclei on a part of the apparently smooth wire surface.

However, certain curious deviations occur for the mixture investigated:

(i) Bubble formation has been delayed to a wire considerably higher critical superheating. Probably, this is caused by large air bubbles, cf. (i).

(iii) In considering the low value of the maximal density of "complex nuclei" m_{max}/A_w for D_w = 100, 50 and 25 μm in comparison to water, one has to keep in mind, that the actual density of active sites is considerably higher.

1.3.2. *Effect of diameter on relative peak flux for horizontal and vertical wires in water–methylethylketone mixtures*

The ratio $q_{m,w,max}/q_{w,p,max}$ for similar wires

in 4·1 wt % methylethylketone and water is shown in Fig. 9 as a function of D_w, for platinum and two different alloys.

The curve for horizontal wires shows a maximum for $D_w = 300$ μm, and approximates a constant value for $D_w > 600$ μm. For very small wire diameters ($D_w \leqslant 25$ μm) premature burnout occurs in both liquids due to the formation of only a small number of vapour bubbles on the heating surface, which results in a low ratio of 1·10. In addition, the data of Fig. 10 reveal, that the actual maximum peak flux in the binary system water—methylethylketone is shifted towards a higher concentration of the more volatile component, i.e. from 4·5 wt % for a 200 μm wire towards 8·0 wt % for a 50 μm wire. This results in too low values of the ratio in Fig. 9 for thin wires. The maximal ratios for $D_w = 50$, 100 and 200 μm following from the data plotted in Fig. 10 are: 2·0, 1·7 and 2·6, respectively. The latter value is in quantitative agreement with previous observations [1, 2].

The low ratio (1·25) for relatively thick wires is probably due to a considerable local exhaustion of the more volatile component nearby the heating surface at peak flux conditions. The curve for vertical wires has been investigated only for $D_w \geqslant 200$ μm and shows a gradually decreasing slope, until a constant ratio of 1·60 is reached for $D_w > 450$ μm. More favourable ratios on vertical wires in comparison to similar horizontal wires are a consequence of the lower peak flux in water for $\phi = \pi/2$ than for $\phi = 0$ (cf. Figs. 2 and 11). This is not the case in the mixture due to the Marangoni-effect.

Figure 10 shows the peak flux for water–methylethylketone mixtures in dependence on liquid composition. For the purpose, to study the indeed very curious curve proposed by Pitts and Leppert [7] for 90 μm Tophet-A (80 Ni; 20 Cr) wires, we investigated the behaviour of of 100 μm Nichrome V (80 Ni; 20 Cr) wires. Pitts and Leppert observed a minimum $q_{w,m,max}$ at 3 wt % methylethylketone, which amounts to approximately 65 per cent of the value in water. A maximum exceeding the value in water with only 10 per cent should occur at 7·5 wt % methylethylketone.

Our results are quite different with exception for the value in water: a maximum peak flux of 2·1 to 2·3 times the value in water occurs (on clean wires and on wires which are slightly oxidized in film boiling, respectively) at 5–12 wt% methylethylketone, a minimum at 3 wt % is not observed at all. The absolute value of the maximum $q_{w,m,max}$ exceeds the corresponding maximum (at 7·0 wt %) for platinum of $D_w = 100$ μm with a factor of 2·0, (2·2 for slightly oxidised Nichrome V wires), and the maximum (at 4·7 wt %) for platinum with $D_w = 200$ μm with a factor of 1·5.

It may be worth noticing, that the transition from nucleate boiling to film boiling can be observed more easily on electrically heated pure metals than on alloys. This is due to the occurrence of a sudden simultaneous decrease in electric current strength and increase in voltage drop caused by the instantaneous increase in the resistance of the wire in case of a pure metal with a considerable temperature coefficient. Sometimes, we observed an intermittent transition from nucleate boiling to film boiling and vice versa on a part of the surface of the Nichrome V wire. This was only the case for heat fluxes approximating the values given in Fig. 10.

To study an eventual effect of the wire diameter, also platinum wires of various diameters have been investigated (Fig. 10). A maximum $q_{w,m,max} = 2{\cdot}0\ q_{w,p,max}$ was observed at 8 wt % methylethylketone for $D_w = 50$ μm; for $D_w = 500$ μm, this ratio amounts to 2·4 at 6–10 wt %. The peak flux on a nichrome V wire with $D_w = 900$ μm increases with increasing concentration of methylethylketone up to a factor of 1·35 at 9 wt%. It was impossible to investigate higher concentrations with those thick wires, as the capacity of the total reflux condenser was insufficient in comparison to the total vapour production rate. The liquid concentrations have now been determined from the boiling-point curve in the equilibrium-diagram. However, a considerable exhaustion of the more volatile component may still occur nearby the heating

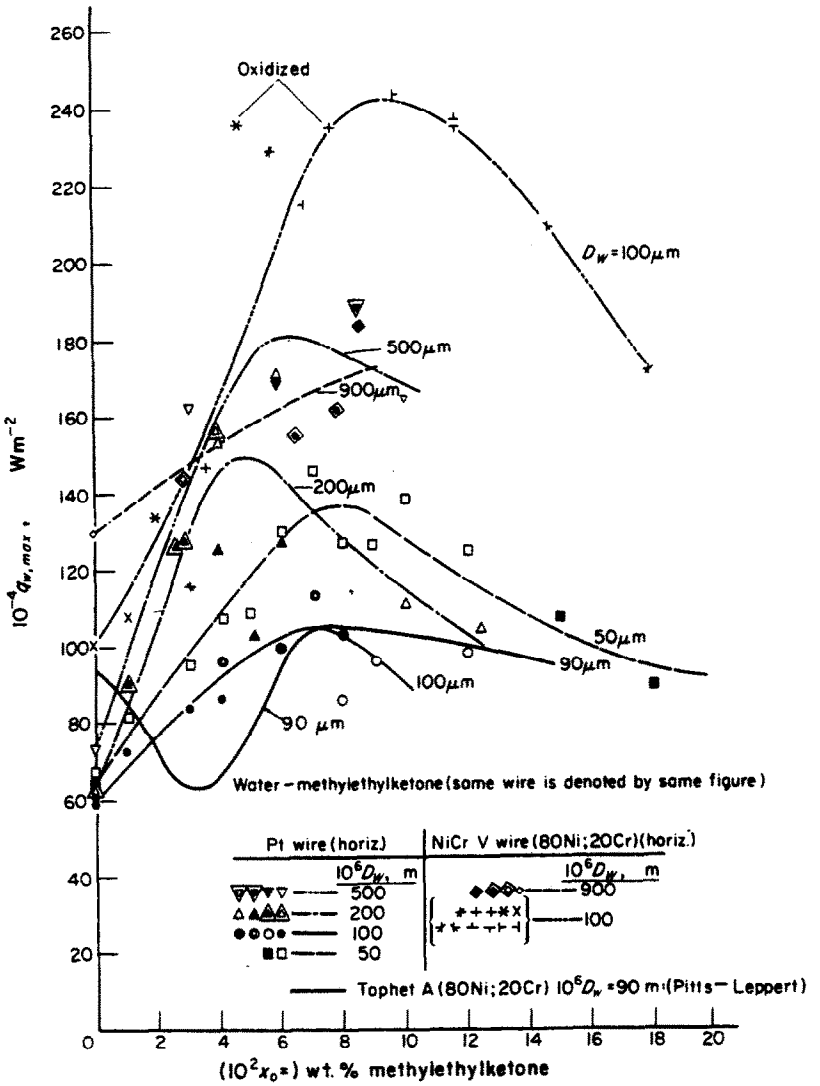

FIG. 10. *Water–methylethylketone.* Nucleate boiling peak flux in dependence on liquid composition for horizontal wires of various diameters.

surface, resulting in a shift of the most favourable concentration towards a higher value.

The general trend of Fig. 7 is confirmed by the data shown in Fig. 10.

2. EFFECT OF ORIENTATION OF HEATING WIRE ON PEAK FLUX

2.1. *Saturated pool boiling*

2.1.1. *Pure liquids*

Figure 11-I shows the nucleate boiling peak flux for water and ethanol on a platinum wire in dependence on the angle ϕ between the axis of the wire and a horizontal plane. The same wire has been used in all experiments for one liquid in order to obtain a better reproducibility of the the results. The peak flux of water on a vertical

wire has been decreased with 28 per cent of the value for a horizontal wire, in good agreement with Fig. 3 (30 per cent), cf. Section 1.2.2.1. For ethanol a similar decrease of 21 per cent occurs.

This decrease is really only due to the presence of a diminished maximal density of active nuclei generating vapour bubbles, as is shown in Fig. 12. The contribution $q_{w,bi,p,max}$, which is predicted to equal the contribution $q_{w,b,p,max}$ due to direct vaporization at the heating surface, but only so in pure liquids [2], is defined by:

$$q_{w,bi,p,max} = q_{w,p,max} - q_{w,co,p,max}. \quad (9)$$

scatter considerably. In addition, the orientation of the wire has no significant influence on the slope of the line. Apparently this means, that active nuclei on both horizontal and vertical wires are similar, i.e. practically, both are generating bubbles of the same size and at a constant frequency on active nuclei.

Actually, one expects that for vertical wires the initial (maximal) thickness of the relaxation microlayer $d_{o,p} = (12/\pi)^{\frac{1}{2}} a^{\frac{1}{2}} t_{1,p}^{\frac{1}{2}} \sim d_{w,co,p} = k\theta_0/q_{w,co,p}$, cf. equation (6) and Section 1.5 of Part II of [2], should be increased in comparison with

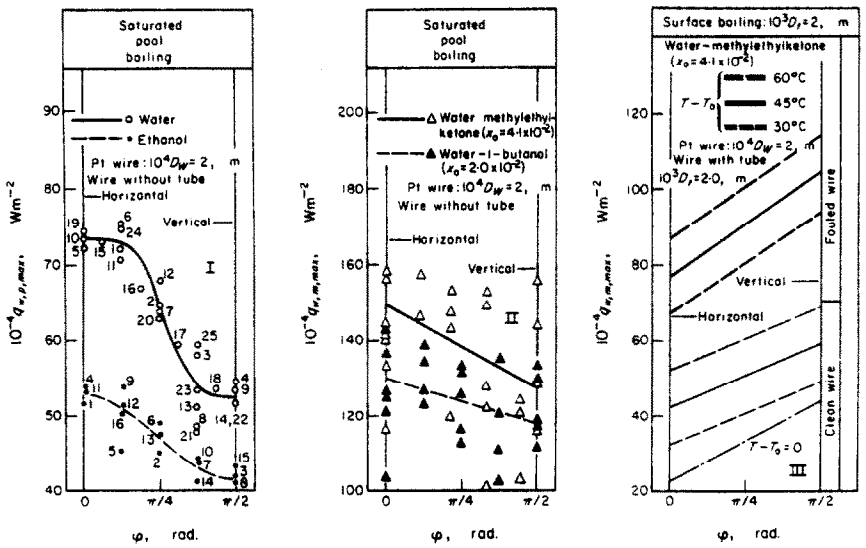

FIG. 11. *Water, ethanol and two aqueous mixtures* in saturated pool boiling, (I, II), and in surface boiling on wire with coaxial glass tube with inner diameter $D_t = 2 \times 10^{-3}$ m, (III), respectively Peak flux in dependence on wire orientation. $L_w = 5{\cdot}20 \times 10^{-2}$ m. (I). Numbers at curves denote sequence of experiments with same wire.

This equals, cf. equation (65) of Part II of (2):

$$q_{w,b,p,max} = \frac{m_{max}}{A_w} \rho_2 l \frac{4\pi}{3} R_{1,p}^3 \nu_p, \quad (10)$$

whence $q_{w,bi,p,max}$ is predicted to be proportial to m_{max}/A_w assuming a constant departure radius $R_{1,p}$ and a constant bubble frequency on all active nuclei.

The experimental results shown in Fig. 12 are in good agreement with this theoretical prediction: the curve can be approximated by a straight line, although the data for different wires horizontal wires (Fig. 11). As a consequence, the departure time t_1 should be prolonged, whence the bubble frequency $1/(4t_{1,p})$ should diminish and the bubble departure radius $R_{1,p}$ should increase according to equation (7). Apparently the resulting effect on $q_{w,p,p} \sim t_{1,p}^{\frac{1}{2}}$ according to equation (10), is only slight.

However, the proportionality $q_{w,bi,p,max} = q_{w,b,p,max} \sim m_{max}/A_w$ is predicted to be valid not only at peak flux conditions, but even in the entire region of nucleate boiling [2]. This important relation is confirmed by the data shown

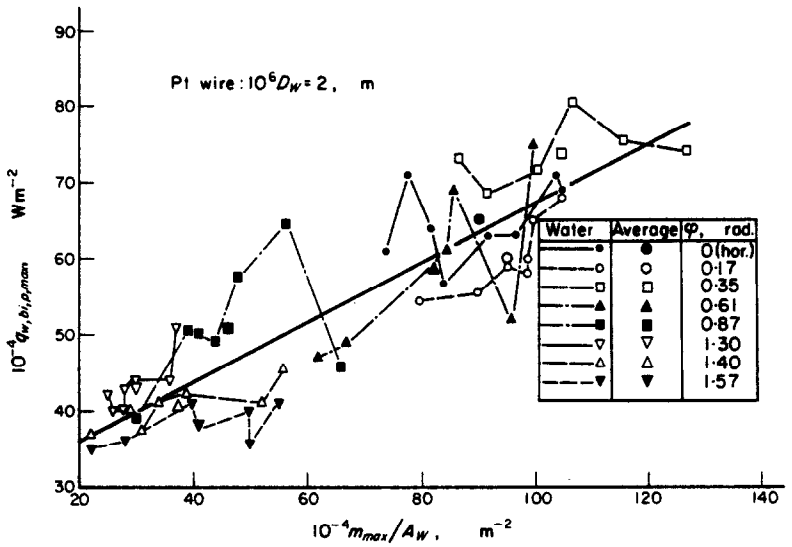

FIG. 12. *Water.* Maximal heat flux above convection at critical conditions in dependence on maximal density of active nuclei for various orientations of platinum wires with $L_w = 3{\cdot}80 \times 10^{-2} - 5{\cdot}60 \times 10^{-2}$ m.

in Fig. 13 both for a horizontal and a vertical wire: the curve $q_{w,bi,p}$ versus m/A_w is represented by a straight line also, cf. Fig. 3. It may be worth reporting, that the slope of the line in Fig. 12 exceeds the slope of the line in Fig. 13 with a factor of 1·8. Obviously, the average product $v_p R^3_{1,p}$ increases at increasing wire superheating θ_0 in nucleate boiling. This effect has been discussed previously, cf. Appendix 3 of Part III of [2].

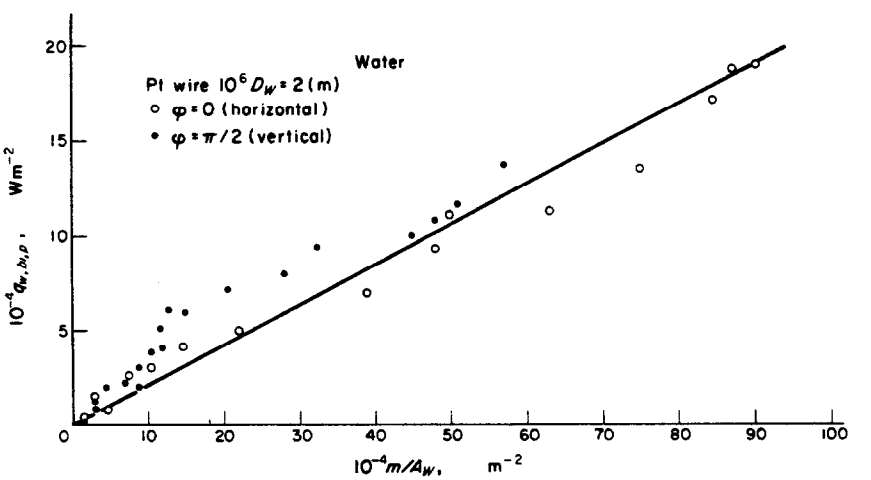

FIG. 13. *Water.* Heat flux above convection in dependence on corresponding density of active nuclei generating vapour bubbles on horizontal and vertical platinum wire with $L_w = 5{\cdot}20 \times 10^{-2}$ m.

Strictly speaking, the results of Figs. 12 and 13 show only, that $q_{w,bi,p} \sim m_{max}/A_w$, whence $q_{w,bi,p} \sim q_{w,b,p}$ in the entire region of nucleate boiling The theoretical identity $q_{w,bi,p} = q_{w,b,p}$ has been checked previously by using a high speed photographic technique for water boiling on a horizontal heating wire, cf. Fig. 1 of Part III of [2]. This relation also holds for $\phi = \pi/2$ (vertical wires) and for $\phi = \pi/4$, as follows from similar experiments (Fig. 14).

Important additional information has been deduced from the high speed motion pictures (Fig. 15):

(i) Both for $\phi = \pi/2$ and $\phi = \pi/4$, the vapour bubbles leave the heating surface perpendicularly. After 11 ms, practically at the instant at which the succeeding bubble is generated on the same nucleus, the bubble is rising upwards. For

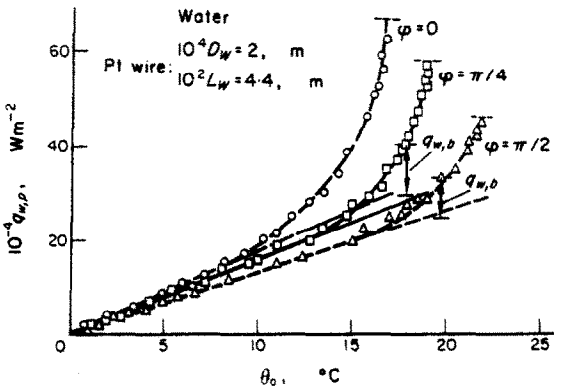

FIG. 14. *Water.* Boiling curves for platinum wires with various orientations at atmospheric pressure. The experimental contribution $q_{w,b}$ of the direct vapour formation at the heating surface (which has been deduced from simultaneous high speed motion pictures), equals the entire increase $q_{w,bi}$ in heat flux density above the corresponding convective contribution $q_{w,co}$.

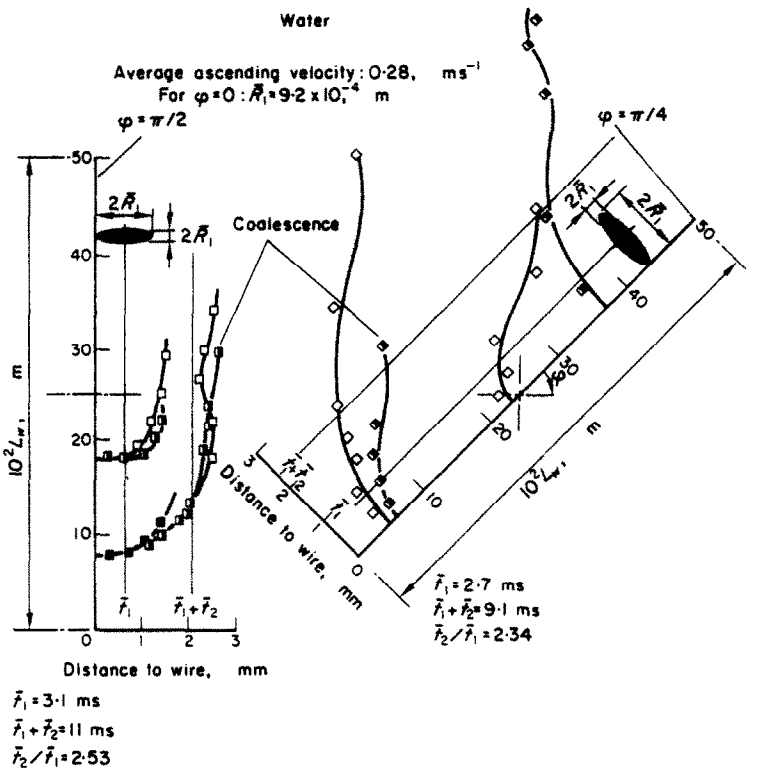

FIG. 15. *Water.* Trajectories of vapour bubbles generated on vertical heating wire ($\phi = \pi/2$ and $\phi = \pi/4$).

$\phi = \pi/2$, the distance of the centre of gravity of the moving bubble to the heating wire is practically constant at approximately 3 mm. This causes a premature onset of local film boiling at the upper end of the wire.

(ii) One has for $\phi = \pi/2$: $\overline{t_1} = 3{\cdot}10$ ms, $\overline{t_2} = 7{\cdot}85$ ms, whence $\overline{t_2}/\overline{t_1} = 2{\cdot}53$, in good agreement with the theoretical value of 3·00 (Section 1.1 of Part II of [2]), which is diminished generally in practice. For $\phi = \pi/4$: $\overline{t_1} = 2{\cdot}74$ ms, $\overline{t_2} = 6{\cdot}40$ ms, whence $\overline{t_2}/\overline{t_1} = 2{\cdot}34$.

(iii) Both for $\phi = \pi/2$ and $\phi = \pi/4$, bubble growth during adherence is in good agreement with Van Stralen's theoretical equation: $R(t) = bC_1\theta_0 t^{\frac{1}{2}} \exp -(t/t_1)^{\frac{1}{2}}$. cf. Section 3.6 of Part I of [2]. The average numerical values of the bubble growth parameter are: $\overline{b} = 0{\cdot}67$ for $\phi = \pi/2$ and $\overline{b} = 0{\cdot}69$ for $\phi = \pi/4$, in comparison with

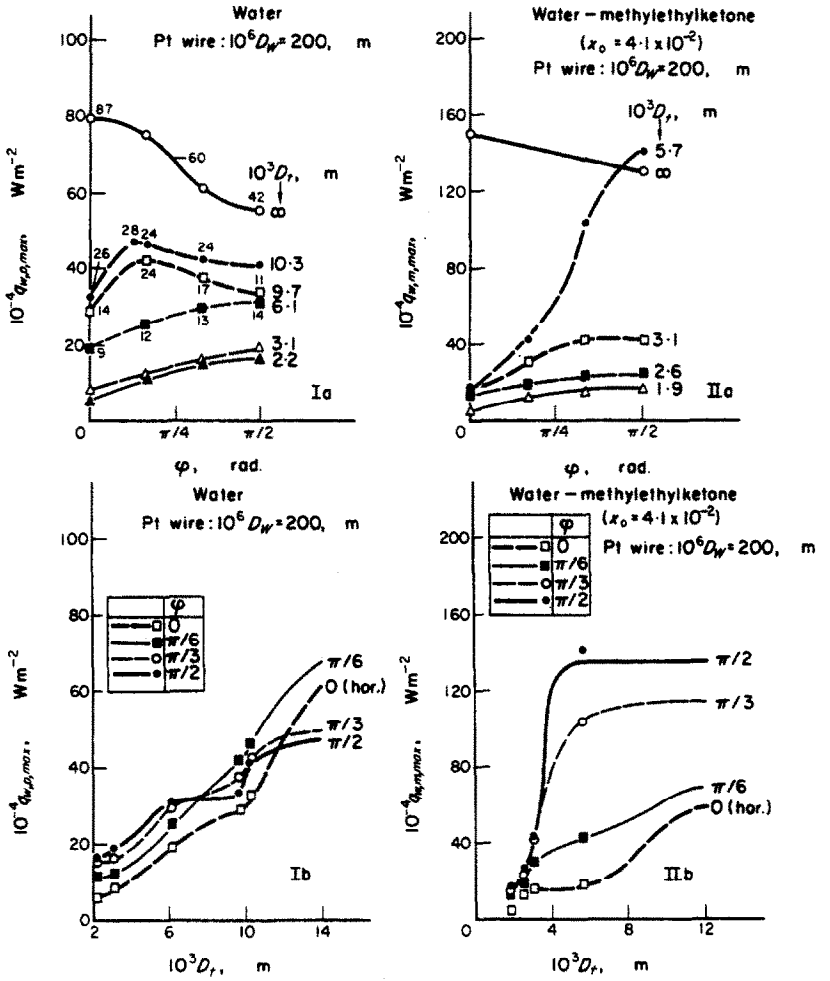

FIG. 16. *Water*, (I), *and water–methylethylketone* (4.1 *wt % methylethylketone*), (II), Peak flux in saturated boiling in dependence on orientation, (I-a and II-a), for various diameters of coaxial glass tube surrounding *platinum* heating wire of circular cross-section. Figures at curves in I-a denote number of active nuclei generating vapour bubbles on a square cm of heating area. Peak flux in saturated boiling in dependence on tube diameter, (I-b and II-b), for various orientations of wire. Curves in I-b (II-b) are deduced from curves in I-a (II-a). $L_w = 5{\cdot}00 \times 10^{-2}$ m; $D_t = \infty$ denotes: wire without tube.

$b = 0{\cdot}71$ for $\phi = 0$ (cf. Section 3.18 of Part I of [2]).

2.1.2. *Binary mixtures*

The average decrease of the peak flux on vertical wires in comparison to the value for horizontal position has been diminished to 11 per cent in binary mixtures containing a low concentration of the more volatile component (Fig. 11-II). This is apparently due to the Marangoni-effect in "positive" mixtures, which minimizes the possibility of bubble coalescence [8, 2, 3]. As a consequence, the favourable effect of obtaining considerably increased peak fluxes in these mixtures, is even more pronounced on vertical wires: for 4·1 wt % methylethylketone in comparison to water, the relative peak flux increases from a factor of 2·05 to a factor of 2·4, and for 2·0 wt % 1-butanol from 1·8 to 2·25.

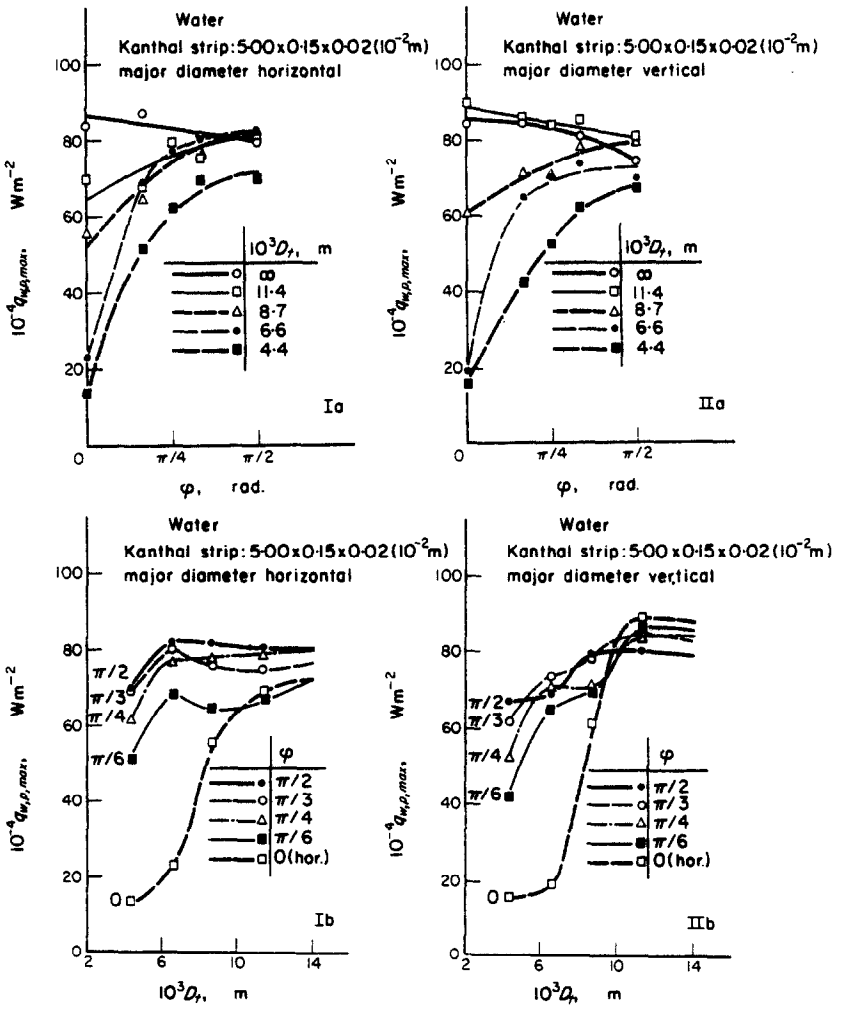

FIG. 17. *Water.* Peak flux in saturated boiling in dependence on orientation, (I-a and II-a), for various diameters of coaxial glass tube surrounding *Kanthal DS* heating strip of rectangular cross-section. Peak flux in saturated boiling in dependence on tube diameter, (I-b and II-b), for various orientations of strip. Curves I-b (IIb) are deduced from curves in I-a (II-a). $L_w = 5{\cdot}00 \times 10^{-2}$ m; $D_t = \infty$ denotes: strip without tube.

2.2. *Surface boiling of binary mixtures on wire with coaxial tube, cf. Section* 4.3

Figure 11-III shows some results for a binary mixture in surface boiling in combination with the effects of orientation and of surrounding the wire with a coaxial tube. The peak flux increases not only with increasing subcooling $T-T_0$ (cf. Part IV of [2]) but also with increasing slope of the wire axis, both on a clean wire and on a fouled wire.

It has been observed previously, that a slight degree of fouling increases the peak flux in saturated boiling, cf. Section 6 of Part III of [2]. Obviously, this effect may under certain conditions be maintained in surface boiling.

It is seen from Fig. 11-III, that the increase in peak flux due to subcooling is only slight in comparison to the case of a wire without tube. One has to keep in mind, that the recorded values of the subcooling have been measured in the bulk liquid, outside the tube. Apparently, a considerable heating occurs of the liquid flowing through the tube. The actual local sub-cooling of liquid in the tube has therefore been diminished considerably. The higher peak flux on vertical wires is also due to the presence of the glass tube: the velocity of the ascending two phase mixture has been increased now, cf. also Section 3.

3. COMBINED EFFECTS OF COAXIAL TUBE AND OF ORIENTATION ON PEAK FLUX IN SATURATED BOILING

3.1. *Water*

Figures 16-I and 17 show the combined effect of placing a coaxial tube around the heating element in water under various orientations for a platinum wire and a Kanthal DS (Fe; Cr; Al; Co) strip, respectively. The peak flux of water boiling on a platinum wire in dependence on orientation decreases in absence of a coaxial glass tube (i.e. $D_t = \infty$), in agreement with Fig. 11-I; this is caused by a considerable reduction of the maximal density of active nuclei generating vapour bubbles (Fig. 16-Ia). Apparently, this effect is of less importance on a Kanthal heating strip (Fig. 17-Ia, IIa). As contrasted with the behaviour of free wires, the peak flux on vertical heating elements ($\phi = \pi/2$) has been increased in case of narrow coaxial tubes (cf. Section 2.2 and Fig. 11-III). As a consequence, the peak flux is approximately independent of orientation in a range of intermediate tube diameters (cf. Figs. 16-Ib and 17-Ib, IIb).

The low value (approximately $10^5 \mathrm{Wm}^{-2}$) for horizontal heating elements ($\phi = 0$), which are surrounded by very narrow tubes, is due to a premature onset of film boiling caused by the presence of only a few vapour bubbles, which cannot escape from the ends of the tube. This value can be deduced from the transition point on the boiling curve between convection and initial nucleate boiling, cf. Fig. 3. A horizontal

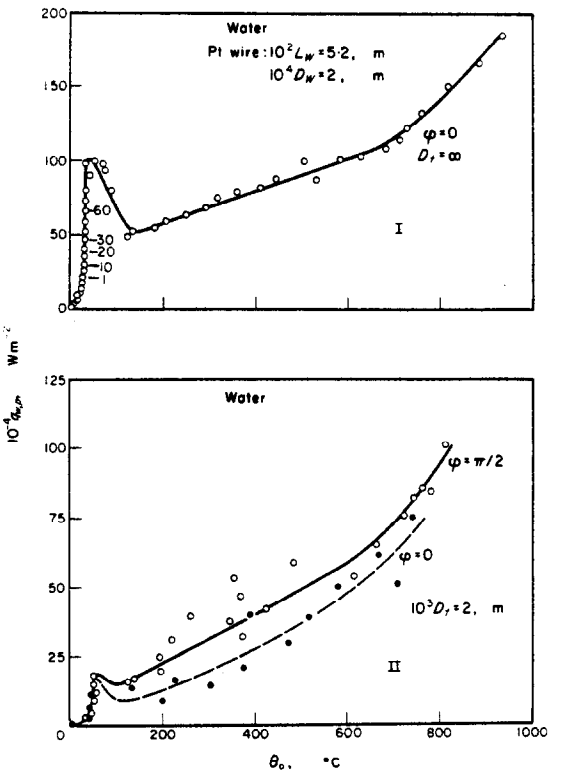

FIG. 18. *Water.* Boiling curves at atmospheric pressure for a horizontal wire without tube, (I), and for a horizontal and vertical wire with coaxial tube, (II). Figures at lower part of curve (I) denote number of active nuclei generating vapour bubbles on a square cm of heating area, cf. Fig. 2.

Kanthal strip ($\phi = 0$) with the major diameter vertical is slightly more favourable compared with the major diameter horizontal, only for a relatively large tube diameter $D_t = 11{\cdot}4 \times 10^{-3}$ m. This is due to the formation of bubbles on the lower side of the strip in the latter case, which have a prolonged departure time. Evidently, corresponding values for $\phi = \pi/2$ must be equal.

The peak flux of major diameter vertical case exceeds even the value on a free wire ($D_t = \infty$) slightly (cf. Fig. 17-IIa). Obviously the introduction of sufficiently wide coaxial tubes has no appreciable influence on the peak flux, even not for horizontal heating elements.

Figure 18-II shows complete boiling curves for water both on a horizontal and on a vertical platinum wire, which is surrounded by a narrow coaxial tube. Figure 18-I shows the corresponding curve for a horizontal wire without tube, also up to the occurrence of a local burnout of the heating element. The corresponding $\theta_0 = 1770 - 100 = 1670$°C is reached indeed only locally, as the average critical value, which has been evaluated from equation (2), amounts to $\bar{\theta}_0 \approx 850$°C. This deviation is due to an axial temperature gradient across the centre and the ends of the wire. Similarly to the behaviour in nucleate boiling, a vertical wire in film boiling, surrounded by a narrow tube is more favourable in comparison to a horizontal wire. In this case, also, the relatively large vapour bubbles generated in film boiling can escape more easily in the vertical position. The heat fluxes are now diminished compared to a wire without tube, with a factor of 6 to 2 at increasing superheating.

3.2. *Binary mixture*

The peak fluxes on a 200 μm platinum wire for the mixture 4·1 wt % methylethylketone are compared with the corresponding values in water at the same tube diameter, cf. Fig. 16-I with Fig. 16-II. The following results are of importance:

(i) Narrow tubes with $1{\cdot}9 \times 10^{-3}$ m $\leqslant D_t \leqslant 3{\cdot}1 \times 10^{-3}$ m: the peak flux in the mixture has increased with a factor of 2 at $\phi = \pi/2$.

(ii) Free wire ($D_t = \infty$): the increase amounts to a factor of 1·9 at $\phi = 0$. The peak flux in the mixture decreases with only 12 per cent at $\phi = \pi/2$ compared with the value at $\phi = 0$, in contradistinction to 30 per cent in water, cf. also Fig. 11-I and Section 2.1.1. This favourable behaviour of the mixture can be attributed to the Marangoni-effect.

(iii) Intermediate interval 6×10^{-3} m $< D_t < 10 \times 10^{-3}$ m: $q_{w,m,\max} = q_{w,p,\max}$ at $\phi = 0$; relatively large bubbles escape from both ends of the tube now, whence the observed independence of peak flux on liquid composition is caused by a considerable exhaustion of the more volatile component inside the tube.

(iv) Intermediate interval at $\phi = \pi/2$: the peak flux in the mixture is equal to the value for $D_t = \infty$, in contradistinction to a corresponding average factor of 0·6 for water (cf. Section 3.3).

3.3. *Discussion*

For nucleate boiling in tubes, we introduce the dimensionless number

$$S = \frac{\frac{1}{2}(D_t - D_w)}{2R_1} = \frac{D_t - D_w}{4R_1}. \tag{11}$$

This number denotes the ratio between the reduced tube radius and the equivalent bubble departure diameter. $S \leqslant 1$ means, that departing bubbles touch the inner tube surface. In this case, hardly any vapour bubble can escape from horizontal tubes. The peak flux is to be expected to increase as $S > 1$ increases.

One has for $D_w << D_t$:

$$S = \frac{D_t}{4R_1}. \tag{12}$$

Roughly speaking, to the neglect of the convective heat transfer, one can state a criterion for the onset of film boiling in tubes for different liquids: the same critical heat flux in tubes occurs at equal values of S.

Obviously, this criterion simplifies the more complex actual situation occurring in some cases, which may be due to various casues, e.g. to a

considerable exhaustion of the more volatile component in horizontal tubes, cf. Section 3.2. The bubble departure radius R_1 depends both on the bubble growth constant $C_{1,p}$ (or $C_{1,m}$ in mixtures) and on the corresponding convective contribution, which determines the departure instant t_1 in equation (7). The average $R_{1,m} = 3{\cdot}4 \times 10^{-4}$ m in 4·1 wt % methylethylketone (Table 3 of Part II of [2]) in comparison to $R_{1,p} = 9{\cdot}2 \times 10^{-4}$ m in water; $C_{1,m} = 0{\cdot}25\, C_{1,p}$ for this mixture. Equal values of S in both liquids are thus obtained for tubes with a 2·7 times smaller inner diameter in the mixture.

corresponding peak fluxes (at the same D_t) on elements of rectangular cross-section exceed the values for circular cross-section considerably up to a factor of 2·5.

Obviously, this is due to the circumstance, that in the latter case a vapour bubble may be surrounded in every direction by neighbouring bubbles, thus having many possibilities for coalescence. Contrarily, in the former case, a bubble generated on a nucleus nearby an edge, can coalesce only with neighbouring bubbles generated at nuclei on the same lateral face. This follows from the fact, that in general bubbles

Table 1. Water and 4·1 wt % methylethylketone. Data at nucleate boiling peak flux on electrically heated platinum wires ($L_w = 5{\cdot}0 \times 10^{-2}$ m; $D_w = 200$ μm) inside vertical tubes of various diameter at constant ratio $S_m/S_p = 2{\cdot}7$

$10^3(D_t - D_w)$ (m)	$10^{-4}\, q_{w,m,max}$ (Wm^{-2})	S_m	$10^{-4}\, q_{w,p,max}$ (Wm^{-2})	S_p	$\frac{q_{w,m,max}}{q_{w,p,max}}$
2·0	21	1·47	16	0·55	1·3
2·9	42	2·13	19	0·79	2·2
5·7	141	4·17	31	1·54	4·5
9·8	141	7·14	37	2·64	3·8

Same data for $\phi = \pi/2$ are collected in Table 1, cf. Fig. 16. Application of the number S seems to be most suitable for vertical tubes, for horizontal tubes use of this number is not successful as stated above, cf. Sections 3.1 and 3.2—(iii).

The peak fluxes are compared in Table 1 at constant D_t and D_w. We compare the critical heat fluxes now at constant values of $S > 1$: $q_{w,p,max} = 31 \times 10^4$ Wm^{-2} for $S_p = 1{\cdot}54$, and $q_{w,m,max} = 21 \times 10^4$ Wm^{-2} for $S_m = 1{\cdot}47$; $q_{w,p,max} = 37 \times 10^4$ Wm^{-2} for $S_p = 2{\cdot}64$, and $q_{w,m,max} = 42 \times 10^4$ Wm^{-2} for $S_p = 2{\cdot}13$. The agreement is reasonably good, if the simplifications underlying the theoretical model are taken into account. It may be worth noticing in this respect, that the influence of the Marangoni-effect is not incorporated in the theory.

Also, an eventual influence of the geometry of the heating element is not yet established sufficiently. It is seen from Figs. 16-Ia and 17-Ia, that, especially in case of the vertical position, the leave the heating surface always perpendicularly (cf. [1, 2, 3] and Section 2.1.1).

This results in a minimized possibility of a premature onset of local film boiling at the upper part of the heating element. A second reason for the occurrence of this effect may follow from the larger heat capacity of the Kanthal strips in comparison to the thin platinum wire used, cf. Section 1.2.4.

4. EFFECTS OF WIRE DIAMETER, OF ORIENTATION AND OF COAXIAL TUBES ON PEAK FLUX IN SURFACE BOILING OF WATER AND BINARY MIXTURES

4.1. *Experimental results for horizontal wires without tube*

The boiling vessel and the experimental procedure have been described previously [3, 9]. Platinum and Nichrome V wires of various diameters have been used.

The most important results are the following:

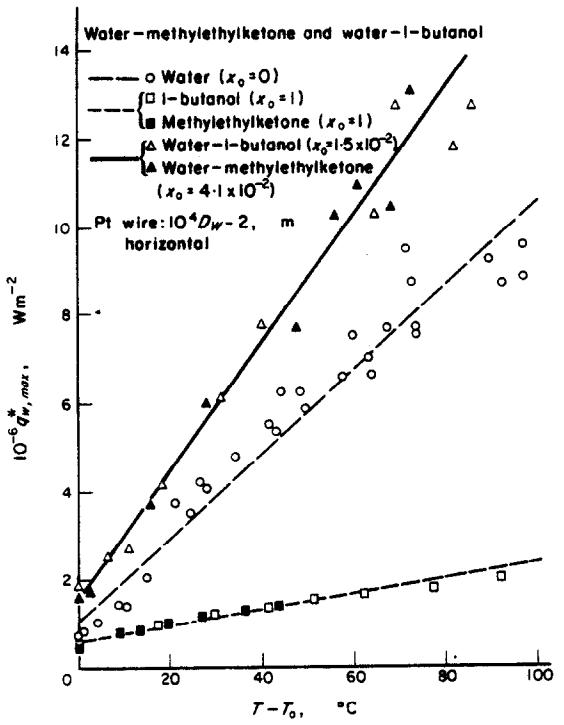

FIG. 19. *Water–1-butanol and water–methylethylketone.* Peak flux in surface boiling with free convection in dependence on subcooling, at atmospheric pressure. The atmospheric boiling point T amounts to: 100 degC (water), 97 degC (1·5 wt % 1-butanol), 118 degC (1-butanol), 88 degC (4·1 wt % methylethylketone) and 80°C (methylethylketone).
The temperature T_0 of the bulk liquid has been measured at a distance of 5 cm to the centre of the heating wire.

(i) The experimental curves $q^*_{w,max}(T-T_0)$ can be represented by straight lines (Figs. 19–23), both for pure liquids and for binary mixtures.

(ii) The ratio $q^*_{w,m,max}/q^*_{w,p,max}$ at constant subcooling $\theta^*_0 = T-T_0$ amounts to approximately 1·50 for aqueous binary mixtures containing the most effective low concentration of the more volatile component (Figs. 19 and 20). This is in quantitative agreement with theoretical predictions (cf. Section 2.2 of Part III of [2]).

(iii) The slope of the curve $q^*_{w,p,max}(T-T_0)$ for 1-butanol and methylethylketone has been diminished to 20 per cent of the value for water (Figs. 19–21).

(iv) The effect of "farberizing" a Nichrome V wire (i.e. oxydizing in film boiling, cf. [10, 1, 2] is slight (15 per cent), and occurs not only in water, but also in aqueous mixtures (Figs. 20–21). This effect is not observed in organic liquids, in agreement with a conclusion, which can be drawn from the extensive research on the nature of this effect by Ogden and Scorah [11].

(v) The slope of the curve $q^*_{w,max}(T_0)$ decreases for increasing wire diameter, D_w (cf. Figs. 20–23).

(vi) The choice of the heating metal has no important effect on the slope of the $q^*_{w,max}(T-T_0)$ curves, provided wires with the same diameter D_w are compared (Figs. 19 and 20).

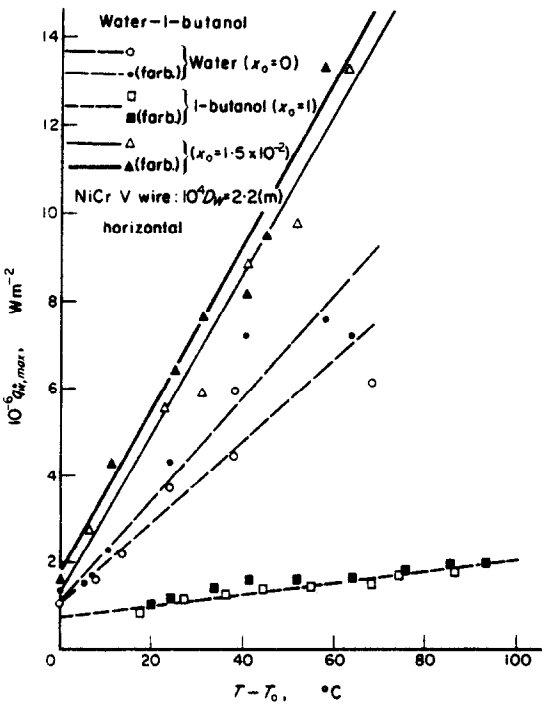

FIG. 20. *Water–1-butanol.* Peak flux in surface boiling with free convection in dependence on subcooling, at atmospheric pressure.
A favourable effect (approximately 15 per cent) of "farberizing" the Nichrome heating wires occurs in water and in aqueous mixtures only, cf. Fig. 21. The temperature T_0 of the bulk liquid has been measured at a distance of 5 cm to the centre of the heating wire.

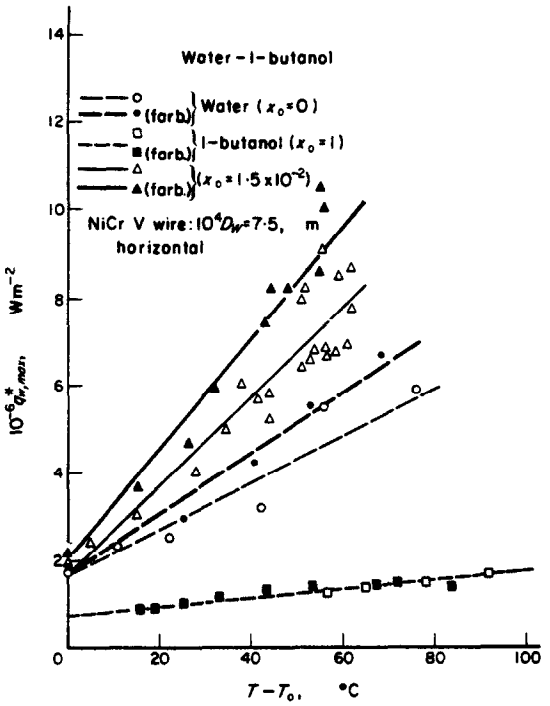

FIG. 21. *Water–1-butanol.* Peak flux in surface boiling with free convection in dependence on subcooling, at atmospheric pressure. The effect of "farberizing" is similar to Fig. 20.
The temperature T_0 of the bulk liquid has been measured at a distance of 5 cm to the centre of the heating wire.

Figure 24 shows the absolute value of the slope of the $q^*_{w,max}(T-T_0)$ lines in dependence on the wire diameter D_w. The following results are of importance here:

(vii) *Organic liquids.* The slope of the curve for the two investigated liquids decreases with only 30 per cent for increasing D_w from 200 μm to 750 μm.

(viii) *Water.* In this range of diameters, a decrease of a factor of 2·1 occurs; in the range from 25 μm to 750 μm, the decrease amounts even to a factor of 3·5.

(ix) *Binary mixtures.* The latter value must be compared with a factor of 1·9 for both aqueous mixtures investigated.

(x) The favourable behaviour of the mixtures in comparison to water diminishes for decreasing wire diameter to zero at D_w = 50 μm, cf. a similar behaviour in saturated boiling on horizontal wires (Fig. 9).

Figure 25 shows the corresponding contribution $q^*_{w,co}(\theta_0 + \theta^*_0)$ of convection to the total heat transfer for water at atmospheric pressure. The lower part of the curves for various diameters tallies with the curves which are shown in Fig. 5. The relative contribution due to forced convection, which is a result of the free convection on the wire in a boiling vessel of limited dimensions, is in surface boiling much lower as in saturated boiling with additional heating of the bottom of the vessel. Comparison of Figs. 25 and 19 for water and D_w = 200 μm yields:

(xi) At large subcoolings, the total $q^*_{w,max}$ is substantially determined by the contribution $q^*_{w,bi,max}$, which is ultimately due to the behaviour of the vapour bubbles.

4.2. *Comparison with theoretical predictions*

A comparison of the results described in Section 4.1 with theoretical predictions is extremely difficult. This is mainly caused by the following:

(i) The temperature T_0 of the bulk liquid has been measured at some distance to the test wire, which is acting as a heat source. This results in too high experimental values of the subcooling $\theta^*_0 = T-T_0$, especially for relatively large diameters D_w and for high subcoolings.

(ii) The peak fluxes may depend both on the diameter D_w and on the orientation of the wire, especially in pure liquids, cf. Section 1.2.2.

At least the results (ii), (v), (vi), (viii) and (xi) of Section 4.1 are in good agreement with Van Stralen's "relaxation microlayer" mechanism (cf. Part IV of [2]), the results (i), (iii), and (vi with Zuber's model [12, 13] which is based on hydrodynamic stability in the region of transition boiling. The Van Stralen theory has the advantage of predicting the behaviour of both the bubble growth and the peak flux in binary mixtures. For pure liquids, an expression for the relative peak flux in pure liquids has been derived, cf. equation (17) of Part IV of [2], which, more generally,

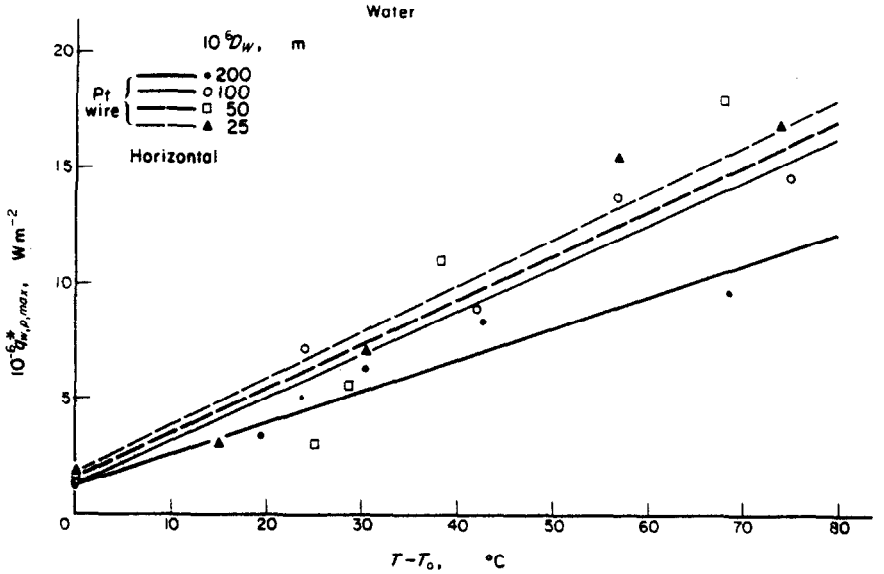

FIG. 22. *Water*. Peak flux in surface boiling with free convection on horizontal platinum wires of various diameters in dependence on subcooling, at atmospheric pressure. The slope of the curve decreases for increasing wire diameter, similar to Fig. 20 in combination with Fig. 21 and to Fig. 23.

The temperature T_0 of the bulk liquid has been measured at a distance of 5 cm to the centre of the heating wire.

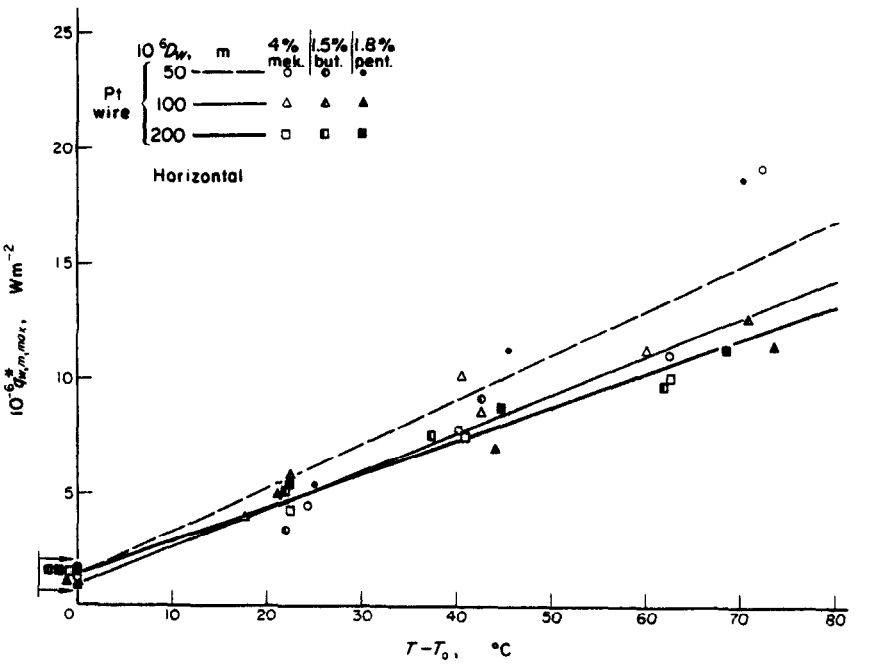

FIG. 23. *Water–1-butanol*, *water–1-pentanol* and *water-methylethylketone*. Peak flux in surface boiling with free convection on horizontal platinum wires of various diameters in dependence on subcooling at atmospheric pressure. The atmospheric boiling point T amounts to: 97 decC (1·5 wt% 1-butanol), 96 degC (1·8 wt% 1-pentanol) and 88 degC (4·1 wt% methylethylketone). The slope of the curve decreases for increasing wire diameter, similar to Fig. 20 in combination with Fig. 21 and to Fig. 22.

The temperature T_0 of the bulk liquid has been measured at a distance of 5 cm to the centre of the heating wire.

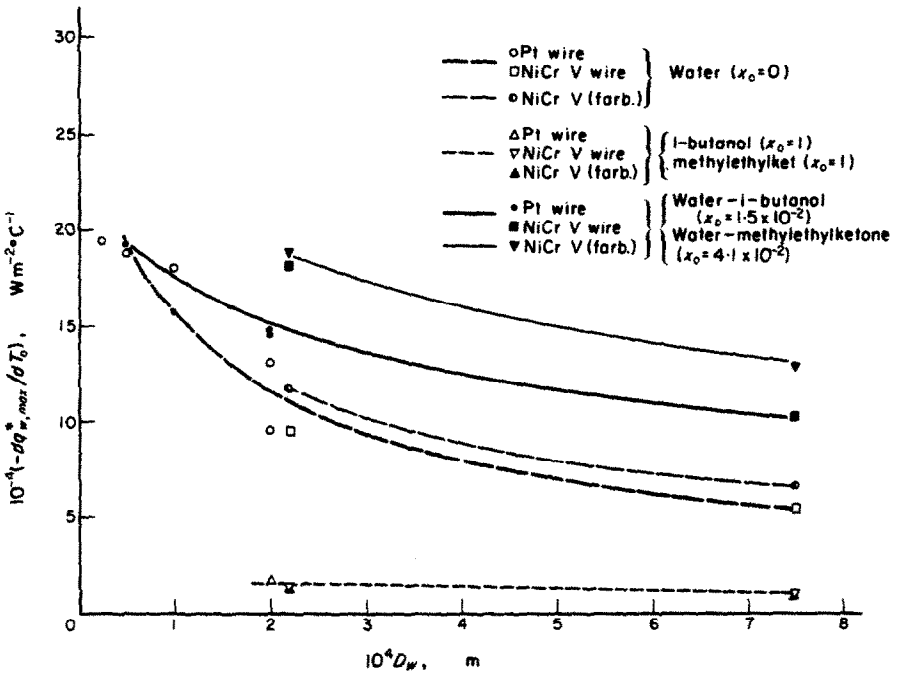

FIG. 24. *Water–1-butanol* and *water–methylethylketone.* Absolute value of the slope of the curves (straight lines) in Figs. 19–23 in dependence on diameter of horizontal heating wire.

can be written as follows:

$$\frac{q^*_{w,p,\max}}{q_{w,p,\max}} = F\left(\frac{\theta_{0,\max} + \theta^*_0}{\theta_{o,\max}}\right) = F\left(1 + \frac{\theta^*_0}{\theta_{o,\max}}\right). \tag{13}$$

Actually, the function F should be quadratic in $\theta^*_0/\theta_{o,\max}$, as a consequence of the rapid increase of $q^*_{w,bi,p,\max}$ at increasing subcooling θ^*_0, cf. equation (9) and equations (13) and (16) of Part IV of [2]. It is shown in Fig. 26, that for the actual $\theta_{o,\max} = 21{\cdot}5$°C, Van Stralen's theoretical ratio $q^*_{w,p,\max}/q_{w,p,\max} = (1/1{\cdot}88)(1 + \theta^*_0/\theta_{o,p,\max})(1 + 0{\cdot}88\,\theta^*_0/\theta_{o,p,\max})$ is in good agreement with the experimental results on thin wires in water at high subcoolings, as might be expected. As a consequence of the above mentioned causes, which result apparently in a linear relation $q^*_{w,\max} \sim \theta^*_0$, cf. the experimental result (i) of Section 4.1, we propose a simple linear expression for the relative peak flux in subcooling:

$$\frac{q^*_{w,p,\max}}{q_{w,p,\max}} = 1 + \frac{\theta^*_0}{\theta_{o,\max}} = 1 + \frac{1}{\theta_{o,p,\max}}(T - T_0), \tag{14}$$

assuming, as previously [2], that $\theta_{o,\max}$ is independent of θ^*_0, cf. [14] and Section 4.3. The Zuber theory [12, 13] predicts also a linear relation, which is obviously caused by assuming a conductive heat transfer mechanism:

$$\frac{q^*_{w,\max}}{q_{w,\max}} = 1 + \frac{24}{\pi}\frac{(k\rho_1 c)^{\frac{1}{2}}}{\rho_2 l}\left[\frac{g(\rho_1 - \rho_2)}{\sigma}\right]^{\frac{1}{4}} \times \left[\frac{\rho_2^2}{\sigma g(\rho_1 - \rho_2)}\right]^{\frac{1}{4}}(T - T_0) = 1 + n(T - T_0). \tag{15}$$

The theoretical factor $24/\pi = 7{\cdot}6$ was replaced by 5·3 in order to obtain quantitative agreement

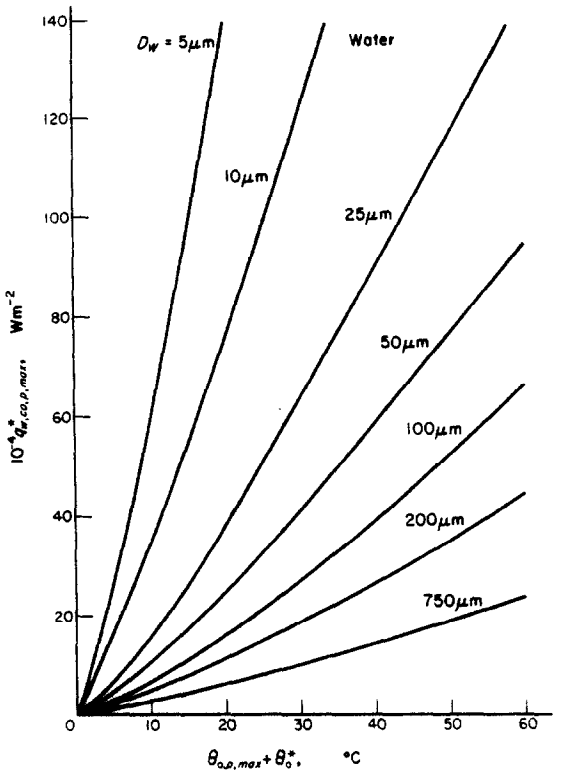

FIG. 25. *Water.* Heat transfer in free convection at atmospheric boiling point on horizontal wires of various diameters, D_w, according to McAdams taking $[D_w]$ as a characteristic dimension, cf. Fig. 5.

with experimental data on subcooled water and ethanol.

Theoretical predictions following from equations (14) and (15) are compared in Table 2 with experimental values. The Zuber theory gives satisfactory results for pure liquids, the predicted absolute values of $q^*_{w,m,max}$ in mixtures are too low; e.g. the theoretical $q^*_{w,m,max} = 9{\cdot}4 \times 10^6$ W/m^2 for 1·5 wt % 1-butanol, and $q^*_{w,p,max} = 9{\cdot}3 \times 10^6$ W/m^2 for water, both at $\theta^*_0 = 100$°C, whence $q^*_{w,m,max} = q^*_{w,p,max}$. Contrarily, the Van Stralen theory [2] predicts a ratio of 1·47 in quantitative agreement with the experimental data. It may be worth reporting, that the simplified equation (14) yields also satisfactory ratios both for pure liquids and for binary mixtures, provided that the same $\theta_{o,p,max}$ is taken instead of $\theta_{o,m,max}$ in the latter case. Quantitative agreement of the absolute heat fluxes in mixtures can be obtained by introducing the factor of 1·47. This factor is based on the effect of slowing down of bubble growth in mixtures. Equating (14) and (15) yields a valuable expression for the critical superheating $\theta_{o,p,max}$ in nucleate boiling:

$$\theta_{o,p,max} = \frac{\pi}{24}\frac{\rho_2 l}{(k\rho_1 c)^{\frac{1}{2}}}\left[\frac{\sigma}{g(\rho_1-\rho_2)}\right]^{\frac{1}{2}} \times \left[\frac{\sigma g(\rho_1-\rho_2)}{\rho_2^2}\right]^{\frac{1}{4}}. \quad (16)$$

The bubble growth constant for pure liquids amounts to [15, 16, 17]:

$$C_{1,p} = \left(\frac{12}{\pi}\right)^{\frac{1}{2}}\frac{(k\rho_1 c)^{\frac{1}{2}}}{\rho_2 l}. \quad (17)$$

Substitution of (17) into (16) yields:

Table 2. Water–1-butanol. *Comparison of experimental and theoretical slope of curve $q^*_{w,max}/q_{w,max}$ in dependence on subcooling at atmospheric pressure. Constant numerical values of the thermal quantities (values at atmospheric boiling point) are assumed*

Liquid	$10^2\, n$ (°C^{-1})				$10^2/\theta_{0,p,max}$ (°C^{-1})	$10^{-4}\, q_{w,max}$ (Wm^{-2})		
			Experimental					
	Zuber, equation (15)		Fig. 19	Fig. 21	Equation (14)	Zuber theory	Experimental	Van Stralen theory
	(factor = 7·6)	(factor = 5·3)	(D_w = 200 μm)	(D_w = 750 μm)			(D_w = 200 μm)	
water	7·52	5·21	9·0	3·3	4·8	109	67	63
1-butanol	5·1	3·1	3·4	1·4	2·9	44	44	33
1·5 wt % 1-butanol	8·4	6·0	9·0	5·2	4·8	100	169	157

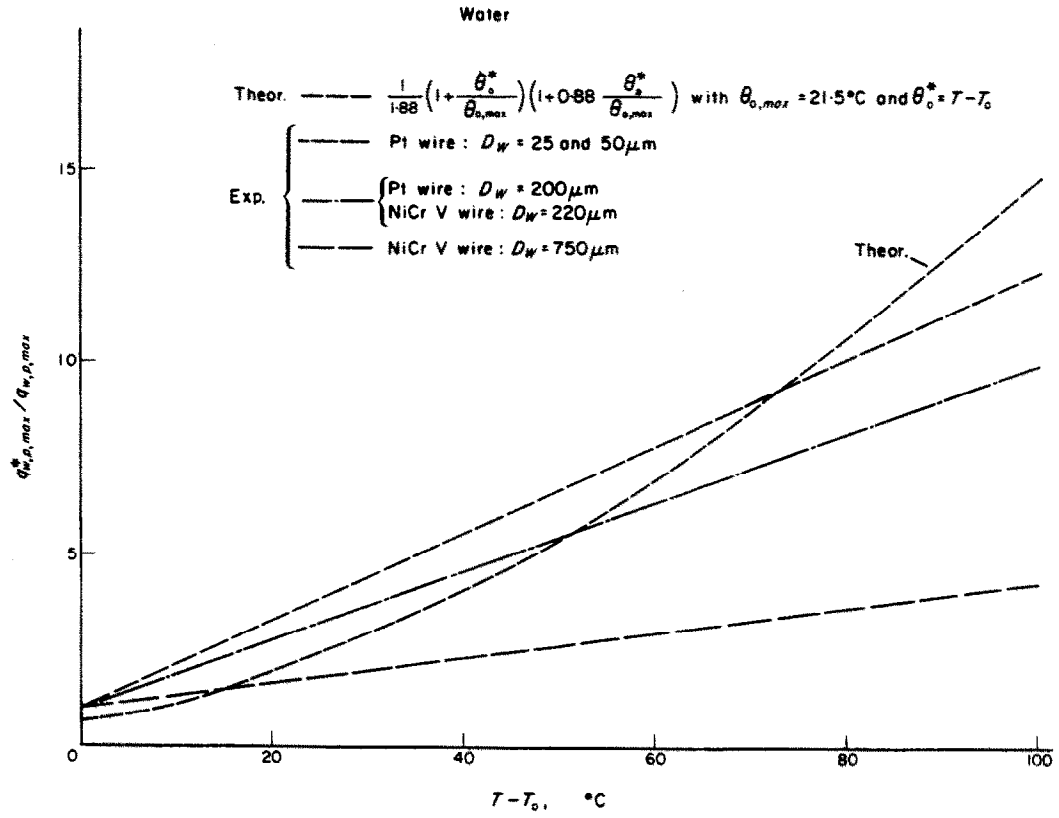

FIG. 26. *Water*. Peak flux in surface boiling on horizontal wires with various diameters in dependence on subcooling. The upper part of the curves for thin wires are in good agreement with Van Stralen's relaxation microlayer theory.

$$\theta_{o,p,max} = \left(\frac{\pi}{48}\right)^{\frac{1}{2}} \frac{1}{C_{1,p}} \left[\frac{\sigma}{g(\rho_1-\rho_2)}\right]^{\frac{1}{2}} \times \left[\frac{\sigma g(\rho_1-\rho_2)}{\rho_2^2}\right]^{\frac{1}{4}}. \quad (18)$$

The critical superheating in binary mixtures with a low concentration of the more volatile component follows from the value in the pure less volatile component by adding an amount $T_p - T_m$[2] at the same values of the parameters. It may be worth noticing, that the derivation of the equations (16) and (18) is semi-empirical.

In equations (16) and (18), the parameter $n = 1/\theta_{o,p,max}$ has been taken. It follows from Table 2, that a better approximation for thin wires in water is obtained by taking $n = 1{\cdot}9$. The effect of the wire diameter can be established by taking $n \sim D_w^{-0{\cdot}50}/\theta_{o,p,max}$, a proportionality, which can be deduced in combination with the results shown in Figs. 4 and 25. Finally, it may be worth reporting, that the ratio $q^*_{w,m,max}(\theta_0^*)/q^*_{w,p,max}(\theta_0^*) = 1{\cdot}47$ is decreased considering $q^*_{w,m,max}(\theta_0^* + \theta_{o,m,max})/q^*_{w,p,max}(\theta_0^* + \theta_{o,p,max})$. However, for 1·5 wt% 1-butanol this correction is not substantial as $\theta_{o,m,max}$ exceeds $\theta_{o,p,max}$ with only 3°C.

4.3. *Effects of orientation and of coaxial tube on peak flux in surface boiling*

In Figure 27-I, the peak flux to water in surface boiling is compared for horizontal (cf. Fig. 22) and vertical platinum heating wires; the latter values were reported by Mosciki and Broder [14]. The critical $\theta_{o,max}$, observed by

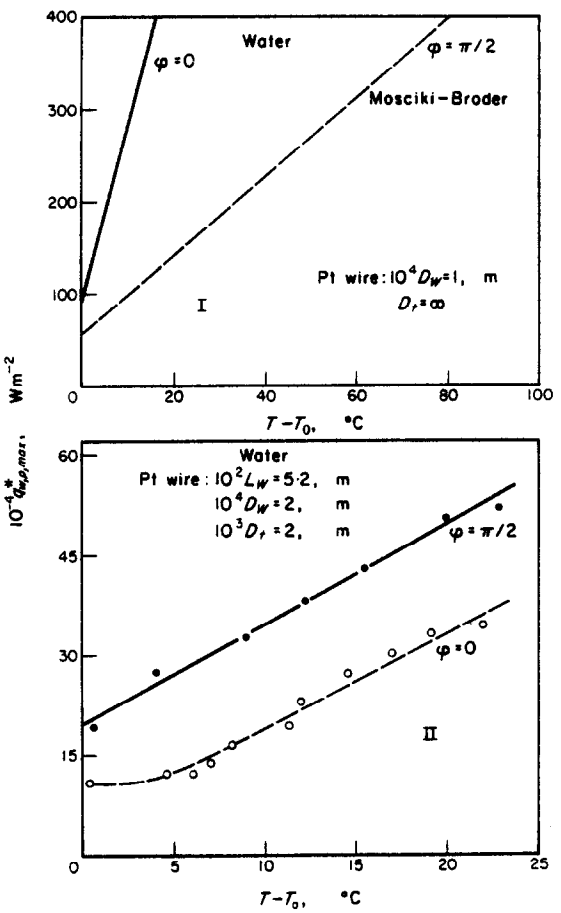

FIG. 27. *Water.* Peak flux in surface boiling with free convection both for horizontal and vertical wires in dependence on subcooling, at atmospheric pressure; (I): wires without tube; (II): wires surrounded by coaxial tube.

these workers, was independent of θ_0^*. Figure 27-II shows the corresponding curves in case of placing a narrow coaxial tube around the wires.

The behaviour is similar to that in saturated boiling of pure liquids:

(i) *Wires without tube*: the peak fluxes on horizontal wires ($\phi = 0$) exceed the corresponding values on vertical wires considerably (up to a factor of 3, cf. Figs. 22 and 27-I).

(ii) *Wires surrounded by a narrow coaxial tube*: the vertical position gives more favourable results; all absolute values are diminished considerably in comparison to case (i). Comparable results of Figs. 27-II and 11-III (Section 2.2) are in good agreement.

It is seen from Fig. 27-II, that for a horizontal wire, the peak flux $q^*_{w,p,\max}$ in surface boiling approximates the value $q_{w,p,\max}$ in saturated boiling already at a subcooling $\theta_0^* = 7°C$. Obviously, this is due to a rapid warming up of the entire quantity of liquid inside the tube to the boiling temperature.

5. THE PEAK FLUX IN SATURATED POOL BOILING OF TERNARY MIXTURES

To our knowledge, no experimental data are known in the literature on the dependence of the critical nucleate boiling heat flux on the liquid composition in aqueous ternary mixtures. Westwater [18] describes results for the non-aqueous system benzene – toluene – xylene by Pelham. The peak flux in the most favourable miscible mixtures exceed the values in the pure excess component with only 20 per cent. This result is in good agreement with the relatively low increase (up to 35 per cent), which can be obtained in organic binary mixtures with a more volatile component. The latter effect has been discussed previously, and is explained by Van Stralen's "relaxation microlayer" theory on the mechanism in nucleate boiling, cf. Section 4 of Part III of [2]. Much higher maxima (up to a factor of 3) occur in aqueous binary mixtures at a low concentration the more volatile component [1, 2]. At this concentration, a maximum $\Delta T/G_d$ occurs, resulting in a maximal slowing down of bubble growth [1,2]; this leads to the "boiling paradox", cf. [2].

5.1. *Water–ethanol–1-butanol*

Figures 28 and 29 show the peak flux at constant mass functions of one of the organic components in dependence of the mass fraction on the remaining organic component. The bottom curves represent $\Delta T/G_d$ for the corresponding aqueous binary systems. The boiling vessel has been described previously [1, 9]. Both the maximum at 3 wt % 1-butanol and the maximum at 12 wt% ethanol in the corresponding binary

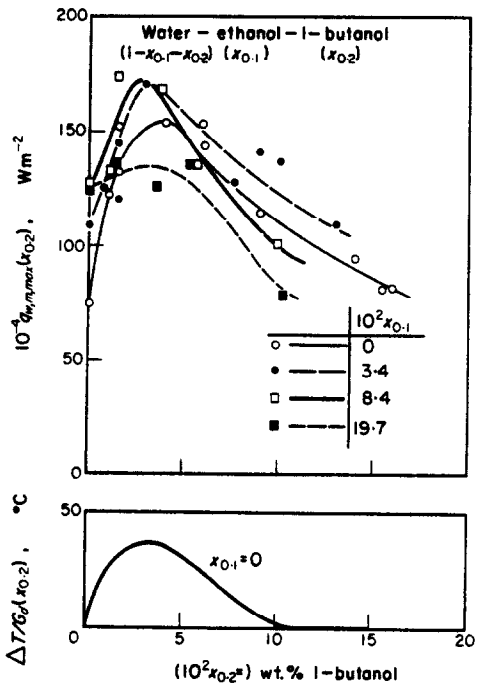

FIG. 28. *Water–ethanol–1-butanol.* Nucleate boiling peak flux on horizontal platinum heating wires ($L_w = 5{\cdot}0 \times 10^{-2}$ m; $D_w = 200$ μm) in saturated pool boiling at atmospheric pressure of ternary mixtures (at various constant mass fractions of ethanol) in dependence on mass fraction of 1-butanol cf. Fig. 29. Bottom curve represents $\Delta T/G_d$ for the binary system water–1-butanol.

systems are increased by adding a suitable quantity of ethanol or 1-butanol, respectively. The mixtures containing 2–3 wt % 1-butanol and 8 wt % ethanol in the range of complete miscibility show the highest maximum, but the increase amounts to only 11% in comparison with the corresponding maximum for 0% ethanol Obviously, the concentrations of this most favourable ternary mixture can be deduced from the $\Delta T/G_d$-curves for the aqueous binary systems.

5.2. *Water–1-butanol–methylethylketone*

Figure 30 shows the peak flux in water–1-butanol–methylethylketone mixtures at constant mass fraction of 1-butanol or methylethylketone, respectively. This ternary system has been chosen, because both basis aqueous binary systems show a very high maximal peak flux at 2 wt % 1-butanol or at 4 wt % methylethylketone, respectively, which exceeds the value in water with a factor of 2·5 [1, 2, 3]. The ternary mixture containing 2 wt % 1-butanol and 4 wt % methylethylketone in the range of complete miscibility shows the highest peak flux indeed, in agreement with the behaviour of the system water–ethanol–1-butanol, cf. Section 5.1. Also, in this case, the increase is restricted to only 15 per cent in comparison with maximal values in the corresponding aqueous binary systems.

Evidently, the relative volatility of both organic components has been decreased for the ternary mixtures in comparison with the binary systems. This follows also from a comparison of the corresponding boiling points in Fig. 31, which shows, that the slope of the $T(x_0)$-curve at constant low mass fraction x_0 diminishes by

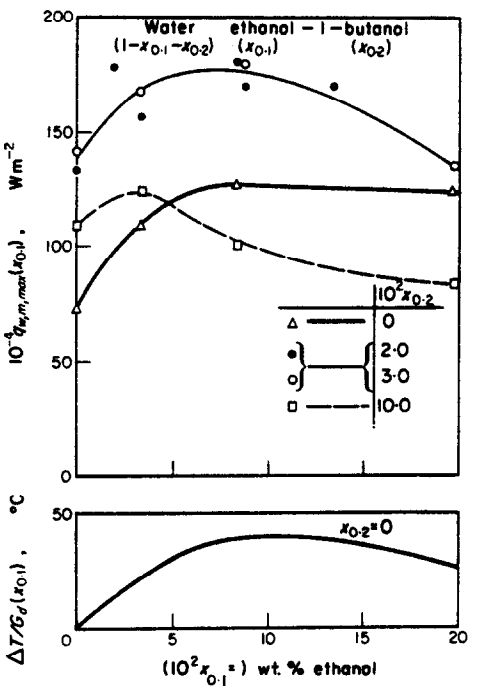

FIG. 29. *Water–ethanol–1-butanol.* Nucleate boiling peak flux on horizontal platinum heating wires ($L_w = 5{\cdot}0 \times 10^{-2}$ m; $D_w = 200$ μm) in saturated pool boiling at atmospheric pressure of ternary mixtures (at various constant mass fractions of 1-butanol) in dependence on mass fraction of ethanol, cf. Fig. 28. Bottom curve represents $\Delta T/G_d$ for the binary system water–ethanol.

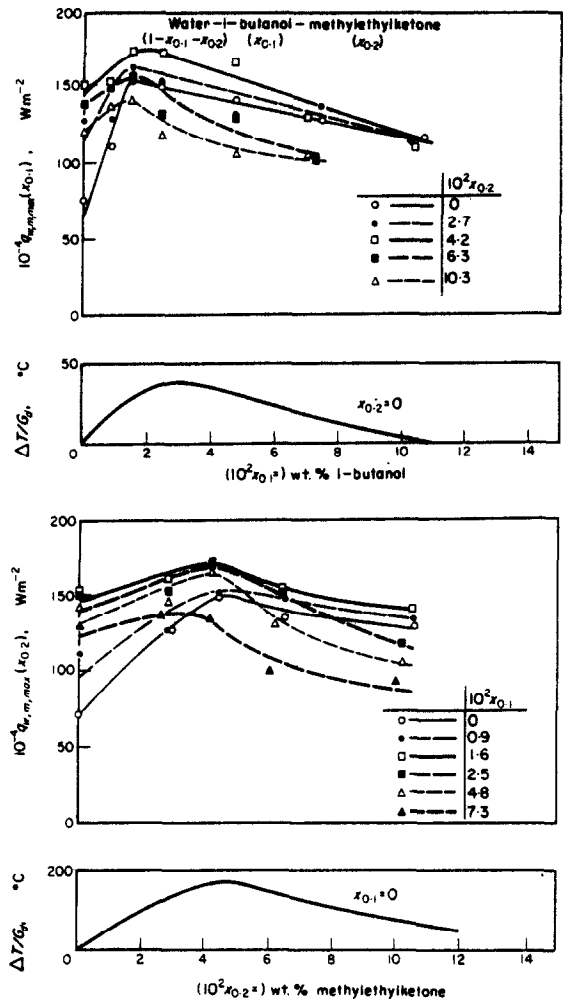

FIG. 30. *Water–1-butanol–methylethylketone.* Nucleate boiling peak flux on horizontal platinum heating wires ($L_w = 5{\cdot}0 \times 10^{-2}$ m; $D_w = 200$ μm) in saturated pool boiling at atmospheric pressure at ternary mixtures at various constant mass fractions of one of the organic components. Bottom curves represent $\Delta T/G_d$ for the basic aqueous binary systems.

adding a third volatile component. The $\Delta T/G_d$-curve for a binary system can be derived graphically from the equilibrium-diagram at constant pressure, whence $\Delta T/G_d$ is dependent on the slope of the $T(x_0)$-curve, cf. Fig. 2 of Part II of [2] and Fig. 7 and equation (73) of Part I of [2]. Consequently, the maximal value of $\Delta T/G_d$ has been decreased in ternary mixtures. But, on the other hand, two (lower) contributions to the total resulting $\Delta T/G_d$ have to be considered. Apparently, this results in a slight increase of the maximal slowing down of bubble growth. Viz., one has the following asymptotic approximation for spherically symmetric bubble growth in initially uniform superheated binary mixtures [2, 3]:

$$R_m(t) \cong C_{1,m}\theta_0 t^{\frac{1}{2}} = \left(\frac{12}{\pi}\right)^{\frac{1}{2}} \times \frac{a^{\frac{1}{2}}}{(\rho_2/\rho_1)[1/c + (a/D)^{\frac{1}{2}}\Delta T/G_d]}. \quad (19)$$

As the numerical value of $(a/D)^{\frac{1}{2}}$ for water–1-butanol and water–methylethyl ketone mixtures at atmospheric boiling point differ only

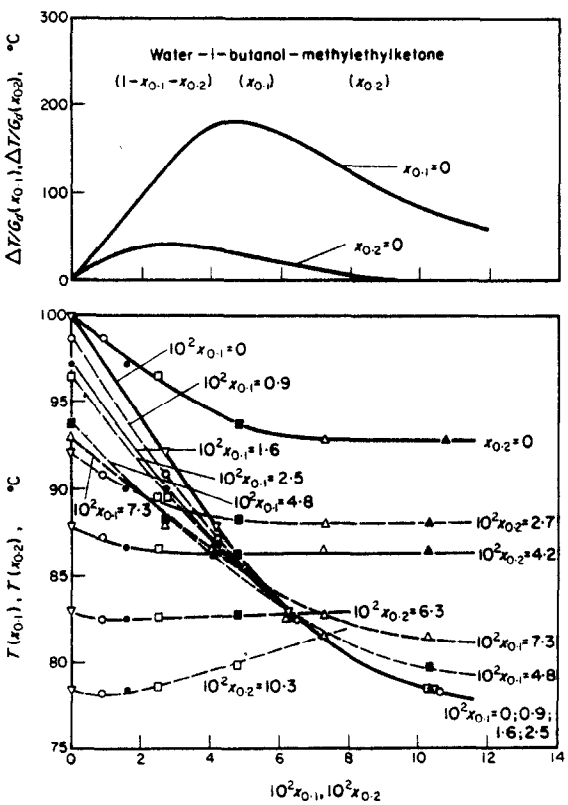

FIG. 31. *Water–1-butanol–methylethylketone.* Boiling-point curves at atmospheric pressure for ternary system at various constant mass fractions of one of the organic components. Bottom curves represent $\Delta T/G_d$ for the basic aqueous binary systems.

2 per cent, one can substitute the total $\Delta T/G_d$ in ternary mixtures into the denominator in the right-hand side of equation (19). Obviously, the resulting maximal $\Delta T/G_d$ in ternary mixtures exceeds both the individual maxima in the basic aqueous binary mixtures, but is smaller than the sum, cf. equation (72) of Part I of [3]. This results in a slightly increased slowing down of bubble growth and hence in an increased peak flux [2] in suitably chosen ternary mixtures compared to binary mixtures.

More exact theoretical predictions may be possible only if complete equilibrium data, including the vapour composition, shall be known in the literature. Also, an eventual dependence of the diffusion constants on concentration may be of some importance.

ACKNOWLEDGEMENTS

The cooperation of Ir. J. Blom concerning recordings of boiling curves on very thin wires, and of J. A. H. Berghs on the photographic technique is gratefully acknowledged.

Thanks are also due to the following graduate students for assistance: J. G. W. H. Lammers, H. F. J. Dohmen, H. P. J. J. Vennekens, J. G. W. van Kampen, J. J. H. Donders, N. J. Chaclin, H. W. P. M. Boreas, J. J. Versmissen, C. J. J. Joosen, E. Janssens, P. F. M. Ooms and C. W. Spoor.

REFERENCES

1. S. J. D. VAN STRALEN, Warmteoverdracht aan kokende binaire vloeistofmengsels, Doctor thesis, Univ. of Groningen, The Netherlands; Veenman, Wageningen, The Netherlands (1959). In Dutch with English summary and captions.
2. S. J. D. VAN STRALEN, The mechanism of nucleate boiling in pure liquids and in binary mixtures—Part I, *Int. J. Heat Mass Transfer* **9**, 995–1020 (1966); Part II, *Int. J. Heat Mass Transfer* **9**, 1021–1046 (1966); Part III, *Int. J. Heat Mass Transfer* **10**, 1469–1484 (1967); Part IV—Surface boiling, *Int. J. Heat Mass Transfer* **10**, 1484–1498 (1967).
3. S. J. D. VAN STRALEN, The growth rate of vapour bubbles in superheated pure liquids and binary mixtures—Part I, Theory; Part II, Experimental results, *Int. J. Heat Mass Transfer* **11**, 1467–1489, 1491–1512 (1968).
4. W. H. MCADAMS, *Heat Transmission*, 3rd Edn, p. 176. McGraw-Hill, New York (1945).
5. B. GEBHART, *Heat Transfer*, p. 270. McGraw-Hill, New York (1961).
6. R. COLE and H. L. SHULMAN, Critical heat flux values at sub-atmospheric pressures, *Chem. Engng Sci.* **21**, 723–724 (1966).
7. C. C. PITTS and G. LEPPERT, The critical heat flux for electrically heated wires in saturated pool boiling, *Int. J. Heat Mass Transfer* **9**, 365–377 (1966).
8. J. HOVESTREUDT, The influence of the surface tension difference on the boiling of mixtures, *Chem. Engng Sci.* **18**, 631–639 (1963).
9. S. J. D. VAN STRALEN and W. M. SLUYTER, Local temperature fluctuations in saturated pool boiling of pure liquids and binary mixtures, *Int. J. Heat Mass Transfer* **12**, 187–198 (1969).
10. E. A. FARBER and R. L. SCORAH, Heat transfer to water boiling under pressure, *Trans. Am. Soc. Mech. Engrs* **70**, 369–384 (1948).
11. P. OGDEN and R. L. SCORAH, The effect of high temperature steam on a nickel-chromium-iron alloy, *Bull. Univ. Mo. Engng Ser.* 38, **53** (16) (1952).
12. N. ZUBER, On the stability of boiling heat transfer, *Trans. Am. Soc. Mech. Engrs* **80**, 711–720 (1958).
13. N. ZUBER and M. TRIBUS, Further remarks on the stability of California, Los Angelos (1958).
14. I. MOSCICKI and J. BRODER, Discussion of heat transfer from a platinum wire submerged in water, *Rosz. Chem.* **6**, 319–354 (1926); M. JAKOB, *Heat Transfer*, Vol. 1, p. 655. John Wiley, New York; Chapman & Hall, London (1950).
15. M. S. PLESSET and S. A. ZWICK, The growth of vapour bubbles in superheated liquids, *J. Appl. Phys.* **25**, 493–500 (1954).
16. H. K. FORSTER and N. ZUBER, Growth of a vapour bubble in superheated liquid, *J. Appl. Phys.* **25**, 474–478 (1954).
17. L. E. SCRIVEN, On the dynamics of phase growth, *Chem. Engng Sci.* **10**, 1–13 (1959).
18. J. W. WESTWATER, Heat transfer to boiling mixtures, Chap. 6 in *Lecture Series on Boiling and Two-Phase Flow for Heat Transfer Engineers* (Edited by H. A. JOHNSON). Univ. of California (1965).

Résumé——Les effets du diamètre et de l'orientation de fils chauffés électriquement sur leur flux de chaleur critique ont été étudiés à la fois en ébullition saturée en réservoir et en ébullition de surface.

Un minimum du flux de pointe sur des fils horizontaux dans l'ébullition saturée se produit pour un diamètre de 100 μm. Le flux de pointe augmente rapidement lorsque le diamètre diminue comme conséquence d'une augmentation correspondante dans le transport de chaleur par convection. Un effet similaire a été observé dans l'ébullition de surface, où la pente du flux de chaleur en fonction des courbes de sous-refroidissement pour des fils horizontaux augmente lorsque le diamètre du fil diminue.

Généralement, le flux de chaleur critique sur des fils horizontaux dans des liquides purs dépasse la valeur

sur des fils verticaux. Ceci est causé par un démarrage prématuré de l'ébullition par film dans le dernier cas par la formation de bouchons de vapeur à l'extrémité supérieure du chauffoir.

Au contraire, les flux de chaleur considérablement plus élevés se produisant dans certains mélanges binaires (en coincidence avec un ralentissement de la croissance des bulles à de faibles concentrations du constituant le plus volatil) sont pratiquement indépendants de l'orientation de l'élément de chauffe, parce que l'effet Marangoni diminue la possibilité de coalescence des bulles.

Un comportement tout à fait différent du flux de pointe est observé sur les fils et les rubans, qui sont entourés par un tube coaxial rapproché: des valeurs élevées se présentent maintenant sur des éléments de chauffe verticaux, car la possibilité pour les bulles de s'échapper de l'intérieur du tube est minimisée dans la position horizontale.

Quelques recherches préliminaires sur le flux de pointe dans l'ébullition saturée en réservoir de mélanges aqueux ternaires montrent l'existence d'une relation directe avec le comportement des mélanges aqueux binaires.

Zusammenfassung—Die Einflüsse des Durchmessers und der Orientierung von elektrisch beheizten Drähten auf den kritischen Wärmestrom bei Behältersieden im Sättigungszustand, sowie bei Oberflächensieden, wurden untersucht. Ein Minimum im Maximalwarmestrom tritt an horizontalen Drähten bei gesättigtem Sieden an einem Durchmesser von 100 μm auf. Bei Verminderung des Durchmessers steigt der maximale Wärmestrom rasch an in Folge eines entsprechenden Anwachsens des konvektiven Wärmetransportes. Ein ähnlicher Effekt wurde beim Oberflächensieden beobachtet, wo die Steigung der Kurven des maximalen Wärmestromes über dem Unterkühlungsgrad für horizontale Drähte mit abnehmendem Drahtdurchmesser zunimmt.

Im allgemeinen übertrifft der kritische Wärmestrom an waagerechten Drähten in reinen Flüssigkeiten den Wert für senkrechte Drähte. Dies wird hervorgerufen durch ein frühzeitiges Einsetzen des Filmsiedens im zweiten Falle, da sich Dampfballen am oberen Ende des Heizdrahtes ausbilden. Im Gegensatz dazu sind die beträchtlich höheren maximalen Wärmeströme in bestimmten Zweistoffgemischen (zugleich verbunden mit einer Verzögerung im Blasenwachstum bei geringer Konzentration der leichterflüchtigen Komponente) praktisch unabhängig von der Orientierung des Heizelementes, da der Marangoni-Effekt die Möglichkeit zum Blasenzusammenwachsen beeinträchtigt.

Ein ganz anderes Verhalten des maximalen Wärmestromes wurde an Drähten und Bändern beobachtet, die von einem engen Rohr koaxial umschlossen waren: die höheren Werte treten nun an den senkrechten Heizelementen auf, da die Möglichkeit für die Blasen, aus dem Rohrinneren zu entweichen, in der waagerechten Lage am geringsten ist.

Einige vorbereitende Untersuchungen über den maximalen Wärmestrom bei gesättigtem Sieden von wässrigen Dreistoff-Lösungen zeigen die Existenz einer direkten Beziehung zu dem Verhalten der grundlegenden Zweistofflösungen.

Аннотация—Исследовалось влияние диаметра и ориентации электрически нагретых проволочек на критический тепловой поток как при насыщенном кипении в открытом объеме, так и при кипении на поверхности.

Минимум критического теплового потока на горизонтальных проволочках при насыщенном кипении достигался при диаметре проволочки 100 μм. С уменьшением диаметра критический тепловой поток быстро увеличивается за счет увеличения доли конвективного теплообмена. Аналогичный эффект наблюдался при кипении на поверхности, когда неклон кривой на графике «критический тепловой поток — кривые недогрева» для горизонтальных проволочек увеличивался с уменьшением диаметра проволоки.

Вообще, величина критического теплового потока на горизонтальных проволочках при кипении чистых жидкостей больше его значения на вертикальных проволочках. В последнем случае это вызывается ранним наступлением пленочного кипения в результате образования паровых пробок на верхнем конце нагревателя. В противовес этому значительно большие критические тепловые потоки в некоторых бинарных смесях (одновременно с замедлением роста пузырька при низких концентрациях более летучего компонента), практически не зависят от ориентации нагревательного элемента, так как эффект Марангони снижает возможность столкновения пузырьков.

Совершенно другое поведение критического теплового потока наблюдается на проволочках и полосках, окруженных узкой коаксиальной трубкой: большие значения имеют место на вертикальных нагревательных элементах, так как при горизонтальном положении удаление пузырьков изнутри трубки затрудняется. Некоторые предварительные исследования критического теплового потока при насыщенном кипении в большом объеме водных трехкомпонентных растворов свидетельствует о существовании прямой зависимости его от поведения основных водных бинарных смесей.